Published in final edited form as:
Biochim Biophys Acta. 2013 August ; 1831(8): 1311–1321. doi:10.1016/j.bbalip.2013.05.001.

Intestinal Caveolin-1 Is Important for Dietary Fatty Acid Absorption

Shahzad Siddiqi[*], **Atur Sheth**[*], **Feenalie Patel**[*], **Matthew Barnes**[*], and **Charles M. Mansbach II**[*,†,1]

[*]Division of Gastroenterology, Department of Medicine, The University of Tennessee Health Science Center 38163

[†]Veterans Affairs Medical Center, Memphis, TN 38104

SUMMARY

How dietary fatty acids are absorbed into the enterocyte and transported to the ER is not established. We tested the possibility that caveolin-1 containing lipid rafts and endocytic vesicles were involved. Apical brush border membranes took up 15% of albumin bound ^{3}H-oleate whereas brush border membranes from caveolin-1 KO mice took up only 1%. In brush border membranes, the ^{3}H-oleate was in the detergent resistant fraction of an OptiPrep gradient. On OptiPrep gradients of intestinal cytosol, we also found the ^{3}H-oleate in the detergent resistant fraction, separate from OptiPrep gradients spiked with ^{3}H-oleate or ^{3}H-triacylglycerol. Caveolin-1 immuno-depletion of cytosol removed 91% of absorbed ^{3}H-oleate whereas immuno-depletion using IgG, or anti-caveolin-2 or −3 or anti-clathrin antibodies removed 20%. Electron microscopy showed the presence of caveolin-1 containing vesicles in WT mouse cytosol that were 4 fold increased by feeding intestinal sacs 1 mM oleate. No vesicles were seen in caveolin-1 KO mouse cytosol. Caveolin-1 KO mice gained less weight on a 23% fat diet and had increased fat in their stool compared to WT mice. We conclude that dietary fatty acids are absorbed by caveolae in enterocyte brush border membranes, are endocytosed, and transported in cytosol in caveolin-1 containing endocytic vesicles.

Keywords

Caveolae; Caveolin-1; Fatty acid; Fat absorption; Detergent resistant membranes; CD36

1. INTRODUCTION

The intestinal absorptive cell, the enterocyte, has no control over the amount of the products of lipolysis of dietary triacylglycerol, fatty acid (FA) and sn-2-monoacylglcyerol (MAG), that are presented to it. Both of these, but especially FA, are disruptive of biological membranes [1]. Post-prandially in humans, FA concentrations in the duodenum have been measured at 28 mM [2], whereas 500 μM FA have been associated with cellular injury [1]. The rate of FA uptake by enterocytes could be limited by the capacity of specific FA transport proteins such as fatty acid translocase (FAT)/CD36, fatty acid binding protein

[1]To whom correspondence should be addressed: Charles M. Mansbach, II, M.D. Room H210, 956 Court Ave., Memphis, TN, 38163, Voice: (901) 448-5813, Fax: (901) 448-7091 cmansbach@uthsc.edu.

plasma membrane (FABPpm), [1] or fatty acid transport protein 4 (FATP4). Although diffusion as well as a number of proteins have been suggested to participate in FA absorption [3] none have been conclusively shown to limit the rate at which FA enters the enterocyte. In the face of the potentially toxic effects of FA, the enterocyte has developed 2 proposed strategies to limit their potentially damaging effects.

The first is to sequester the FA by their binding to the abundant 2 fatty acid binding proteins expressed by the intestine, liver (FABP1) and intestinal (FABP2) fatty acid binding proteins [4]. The second mechanism is to quickly convert the FA to the physico-chemically inert TAG. TAG synthesis has been observed to be a rapid reaction; within 30 sec,79% of absorbed FA are converted to TAG in rat intestine [5].

The inability to clearly define either diffusion or transport proteins as essential for FA uptake into enterocytes despite much effort suggests the possibility of a mechanism other than what has previously been proposed. One potential recently explored is that of lipid rafts. Lipid rafts are cholesterol-sphingomyelin rich domains in cellular membranes, 10–200 nm in diameter [6], comprising up to 30 to 50% of the membrane surface. Specifically, lipid rafts have recently been shown to cover 50% of the surface of intestinal microvillus membranes [7]. One protein associated with lipid rafts is caveolin of which there are 3 family members, caveolinl-3, each of which is expressed in the intestine [8]. Caveolin has long been known to bind long chain FA [9] and more recently it has been shown to be important for FA uptake into cells [10, 11]. In addition, gene disrupted mice deficient in caveolin-1 have a lean body habitus and have reduced fat stores on a high fat diet as compared to WT mice [12 resistant to diet-induced obesity, and show hypertriglyceridemia with adipocyte abnormalities]. In sum these data strongly suggest that caveolae may be associated with FA uptake into cells and potentially into enterocytes.

Caveolae are associated with a variety of proteins other than caveolin including GPI linked proteins, cell signaling proteins, and a variety of receptors such as epidermal growth factor (EGF) [13]. Important for lipid absorption, FAT/CD36 is also present in lipid rafts [14]. Caveolin-1 is required for FAT/CD36 to be present in the rafts at least in mouse embryonic fibroblasts [11] and potentially enterocytes. One function of FAT/CD36 is as an FA translocase [15]. In support of this mechanism for FA uptake in the intestine, intestinal cells isolated from CD36 KO mice have a 50% reduction in FA uptake [16] resulting in a reduction in chylomicron TAG output by the intestine [17]. Not all investigators agree with these data, however [18].

A third protein associated with caveolae is the glycosylphosphatidylinositol (GPI) linked intestinal alkaline phosphatase (IAP) [19, 20]. Since IAP is known to increase in the mesenteric lymph after a fat meal [21], it was presumed that this was associated with fat absorption. However, when lymphatic chylomicron output was blocked by the non-ionic detergent, pluronic L-81, the increase in lymphatic alkaline phosphatase in response to fat feeding was maintained despite the absence of lymph chylomicron production[22]. The disassociation of IAP from chylomicron secretion was recently confirmed in IAP gene disrupted mice. In these mice, dietary lipid was absorbed as lipid droplets that bypassed the

[1]**Abbreviations**

The abbreviations used are: TAG, triacylglycerol; FA, fatty acid; MAG, sn-2-monoacylglycerol; FAT, fatty acid translocase; CD36, cluster of differentiation 36; FABPpm, Fatty acid binding protein plasma membrane; FABP1, liver fatty acid binding protein; FABP2, intestinal fatty acid binding protein; WT, wild type; KO, knockout; GPI, glycosylphosphatidylinositol; IAP, intestinal alkaline phosphatase; ECL, enhanced chemiluminescence; FATP4, fatty acid transport protein 4; PBS, phosphate buffered saline; MBC, methyl β cyclodextrin; ACSL, acyl-Co-A synthetase long chain; DRM, detergent resistant membranes; DSF, detergent soluble fraction; EM, electron microscopy; BB, brush border; CEV, caveolin-1 containing endocytic vesicles.

Golgi resulting in the more rapid appearance of TAG in the plasma than chylomicrons in WT miJe [23].

In this report we present data suggesting that dietary FA are associated with caveolae in the brush border (BB) of intestinal absorptive cells and remain associated with the caveolae in caveolin-1 containing endocytic vesicles (CEV) in the cytosol.

2. Materials and methods

2.1 Materials

Oleic acid (9.2 Ci/mM) and ^{3}H-cholesterol were obtained from Perkin Elmer Life Sciences. Sephacryl S-100 High Resolution gel filtration medium (Sephacryl S-100 HR) was purchased from GE Healthcare (Piscataway, NJ). Iodixanol (Optiprep) was purchased from Axis-Shield, Plc (Greiner-Bio-One, Longwood, FL). Enhanced chemiluminescence (ECL) reagents were procured from GE Healthcare. Protease inhibitor cocktail tablets were obtained from Roche Applied Science. Immunoblot reagents were purchased from Bio-Rad. Other biochemicals used were analytical grade from Sigma (Sigma Chemical Co., St. Louis, MO) or local companies. Male Sprague Dawley rats, 150–200 g were purchased from Harlan Laboratories (Indianapolis, IN). Caveolin-1 gene disrupted mice (strain: B6.Cg-CavltmlMls/J) and wild type mice (WL) of the same genetic background, C57BL6, were obtained from the Jackson Laboratories (Bar Harbor, ME). Mouse chow containing 23% (w:w) diet in pellet form was obtained from Harlan Laboratories.

2.2 Antibodies

Rabbit polyclonal antibodies against CD36, caveolin-1, caveolin-2, and goat polyclonal antibodies against rabl1 and IAP and mouse anti-caveolin-3 monoclonal antibodies were all purchased from Santa Cruz Biotechnology (Santa Cruz, CA). Clathrin rabbit polyclonal antibodies were purchased from Novus Biologicals (Littleton, CO). FALP4 rabbit polyclonal antibodies were procured from abcam (Cambridge, MA). Antibodies against purified rat FABP1 and 2 were a generous gift of Dr. Judith Storch (Rutgers University, New Brunswick, NJ). Goat anti-rabbit IgG, goat anti-mouse IgG, and rabbit anti-goat IgG conjugated with agarose beads were purchased from Sigma Chemical Co., St. Louis, MO. Goat anti-rabbit IgG, goat anti-mouse IgG, and rabbit anti-goat IgG conjugated with horseradish peroxidase (HRP) were also procured from Sigma.

2.3 Preparation of cytosol from enterocytes isolated from proximal intestinal sacs exposed to ^{3}H-oleate

Cytosol was prepared from rats as previously [24] and from mice following the same protocol. In brief, intestinal sacs from the proximal 1/2 intestine were exposed to 80 μg of Lriacin C for 15 min then to 1 mM ^{3}H-oleate (100×10^{6} dpm) bound to albumin for 2 min and enterocytes isolated [25]. Lhe cells were homogenized and the cytosol obtained by differential centrifugation. The cytosol was not contaminated with mitochondria or ER and only 7% with BB (Lable 1, sucrase). Glucose-6-phosphate dehydrogenase is a cytosolic enzyme so its concentration in cytosol is expected.

2.4 Preparation of BB from intestinal cells of rats and mice

The proximal half of the intestine of either rats or mice, was opened lengthwise, the mucosa obtained by scraping with a glass slide, and placed into 300 mM mannitol, 12 mM Tris-HCl, pH 7.1 (1 g wet wt mucosa in 3 ml buffer). The mucosa was homogenized in a Potter Elvehjem homogenizer and the protocol of Kesser et al. [26] followed to obtain brush borders. 3 rats or 10 mice were used for each preparation. Each preparation was tested for alkaline phosphatase activity and compared to the activity of the whole homogenate.

2.5 The distribution of ^{3}H-oleate incubated with or without BB in an OptiPrep gradient

^{3}H-oleate (0.5 mM, 150,000 dpm) was incubated with 1 mg prot BB isolated from WT or KO mice or by itself at 37°C for 30 min. The BB were washed twice in PBS, re-isolated by centrifugation, and dissolved in 1% Triton X-100. The resulting mixture was placed at the bottom of an OptiPrep gradient [27] and centrifuged for 20h. The gradient was resolved, 1 ml fractions collected starting at the top of the gradient (9 ml total volume), and the total ^{3}H-oleate-dpm determined for each fraction.

2.6 Uptake of ^{3}H-oleate or ^{3}H-cholesterol into native or cholesterol depleted BB

BB from rats or mice, 200 μg protein, were suspended in 200 μl of Dulbecco's Modified Eagle Medium (DMEM) and incubated with DMEM or 20 mM methyl β cyclodextrin (MBC) in DMEM for 60 min at 37°C [28]. The BB were pelleted by centrifugation for 10 min at 4°C, the supernatant discarded, and 200 μl of DMEM added. The BB were washed twice more with 200 μl of fresh DMEM and suspended in 200 μl DMEM. 300 μl of 0.5 mM oleic acid supplemented with 150,000 dpm ^{3}H-oleate bound to 0.2% albumin was added and the suspension incubated for 30 min at 37°C. The suspension was centrifuged for 10 min at 4°C to pellet the BB and the supernatant removed. The BB were washed twice with 500 μl PBS. The supernatant was removed and the BB suspended in 200 μl PBS. The total dpm was taken as the radioactivity of the two combined supernatants plus the BB. BB ^{3}H-oleate uptake was calculated by dividing the dpm of the BB by the total dpm. ^{3}H-cholesterol (50 μM, 220,000 dpm) bound to 0.2% albumin was incubated with BB isolated from KO or WT mice. The BB were incubated for 30 min at 37°C and the BB isolated by centrifugation and washed twice with PBS. The BB were re-suspended in 500 μl of PBS and 50 μl obtained for determination of radioactivity. The percentage uptake by the BB was calculated by determining the total dpm in the supernatant and BB and dividing the dpm in the BB by the total ^{3}H-cholesterol present.

2.7 Isolation of CEV by OptiPrep gradient centrifugation

CEV were isolated from cytosol (1 mg prot) treated with 1% Triton X-100 using the OptiPrep density gradient method as suggested by Harder et al [27]. The cytosol was placed at the bottom of the gradient and the gradient centrifuged. The gradient was resolved by collecting nine 1 ml fractions using a pipette starting at the top of the gradient. 100 μl from each fraction was obtained for radioactivity determination. The proteins in each fraction were precipitated with trichloroacetic acid (TCA), washed with cold acetone, and suspended in Laemmli's buffer. The proteins were separated by SDS-PAGE and identified by immunoblot using specific antibodies as indicated.

2.8 Isolation of CEV by gel-filtration chromatography

1 mg of cytosol treated with 1% Triton X-100 for 5 minutes was applied to a Sephacryl S-100 HR column (1.5 cm × 45 cm) previously equilibrated with 1% Triton X-100 in PBS at pH 7.2 as suggested by Radeva and Sharom [29]. The cytosol was eluted with 1% Triton X-100 in PBS (pH 7.2) at 4°C. 1 ml fractions were collected and 100 μl used for radioactivity determination. The proteins in each fraction were precipitated with TCA, washed with cold acetone, and suspended in Laemmli's buffer. 40 μg protein from each fraction was separated by SDS-PAGE and analyzed by immunoblot using specific antibodies as indicated.

2.9 Measurement of body weight and stool fat excretion of mice on a high fat diet

C57BL6 and B6.Cg-CavltmlMls/J mice (3 weeks old) were maintained in metabolic cages, 2 mice per cage, for 1 week prior to the administration of the test diets. The mice were weighed and then fed either mouse chow or mouse chow supplemented with soybean oil,

2%, and milk fat, 21 %, (23% fat w:w) for 7 weeks. Stool for analysis was obtained on days 7 to 9 of the diet. The mice were weighed weekly. The stools were air dried to a constant weight, powdered, and extracted [30, 31]. The stool was left in contact with the organic phase overnight and washed with 0.1 N HC1. The phases were separated by centrifugation and the organic phase obtained, dried using N2, and the amount of lipid obtained gravimetrically.

2.10 Distribution of ^{3}H-oleate in WT and KO mice after corn oil gavage

WT and caveolin-1 KO mice were anesthetized and gavaged with 0.2 ml corn oil containing 4×10^{6} dpm ^{3}H-oleate. 30 min later, the mice were euthanized and the contents of the stomach were collected and homogenized in 10 ml PBS. The intestine was removed and the luminal contents obtained by flushing the intestine with 10 mM taurocholate in PBS (10 ml). The remaining intestine and cecal contents were homogenized separately in 10 ml PBS. All fractions were kept on ice. 100 μl of each fraction was obtained for determination of ^{3}H-dpm.

2.11 SDS-PAGE Gel electrophoresis and Immunoblots

Proteins were separated by SDS-PAGE, transblotted to nitrocellulose membranes (Bio-Rad), blocked with 5% Blotto and the membranes incubated with specific primary antibodies. After adding peroxidase-conjugated secondary antibodies, the labeled proteins were detected using ECL (Amersham Biosciences).

2.12 Electron microscopy

Cytosol was prepared as above from mouse or rat proximal jejunal sacs incubated with or without albumin bound 1 mM oleate. Cytosolic vesicles were visualized by negative staining [24]. Immunogold labeling of vesicles was performed as described [24].

2.13 Immuno-depletion of proteins from cytosol

Immuno-depletion of specific proteins from intestinal cytosol was accomplished by incubating cytosol (1 mg) with 20μl anti-caveolin-1 antibody at 4°C for 4 h. 40 μl of anti-rabbit IgG bound to agarose beads (Sigma Chemical Co.) were added and incubated for another 4 h at 4°C. The beads were collected by centrifugation and discarded. The supernatant was retained. This process of antibody depletion was repeated twice more. Caveolin-2, −3, IAP, FAT/CD36, and clathrin were similarly immuno-depleted using their specific antibodies and anti-IgG bound agarose beads. Samples from each round of immuno-depletion for each antibody were obtained for immunoblotting.

2.14 Co-hnmuno-precipitation of proteins from cytosol

Immuno-precipitation of proteins from intestinal cytosol was accomplished by incubating cytosol (1 mg protein) with 20 μl antibodies generated in rabbits to caveolin-1, FAT/CD36, or IgG and generated in goats to IAP at 4°C for 4 h. 40 μl of anti-rabbit (goat) IgG bound to agarose beads (Sigma) were added and incubated for another 4 h at 4°C. The beads were collected by centrifugation, washed ten times with cold PBS, and immunoblots performed using antibodies to caveolin-1, IAP, and FAT/CD36.

2.15 Cholesterol and alkaline phosphatase measurement

Alkaline phosphatase was measured by the rate of release of p-nitrophenol from p-nitrophenol phosphate. Cholesterol was measured using the Infinity Cholesterol Estimation Kit from Sigma Chemical Co. as directed.

Statistical Analysis—Comparisons between means were carried out using a statistical package supplied by GraphPad Software (Instat, GraphPad Software, Inc, San Diego, CA) using a two-tailed t test or the statistical package supplied with Excel (Microsoft Excel for Mac 2011, version 14.3.1).

2.16 Study approval

Animal studies were approved by the University of Tennessee Health Science Center Institutional Animal Care and Use Committee, #293 and 1563 and are in accord with NIH guidelines for humane treatment of laboratory animals.

3. RESULTS

3.1 Intestinal brush border membranes take up dietary FA in caveolae

We first wished to test the functionality of intestinal BB in dietary FA uptake by determining if mouse BB could compete for ^{3}H-oleate bound to albumin. Our BB preparation had 17 fold greater alkaline phosphatase activity than whole cells (114 nmol/mg prot/min vs. 7.4 nmol/mg prot/min respectively). After 30 min incubation of BB with albumin- ^{3}H-oleate, ≈15% partitioned into the BB (Fig. 1A, WT), possibly lipid rafts (detergent resistant membranes [DRM]). As a first test of this potential, we used cholesterol depletion of BB by MBC. MBC treatment reduced BB cholesterol by 43% (293 ± 31 vs. 170 ± 19 μg cholesterol/mg BB prot) but oleate uptake was reduced 95% (Fig. 1 A, WT-dep). MBC treated cells incorporated 55% of absorbed ^{3}H-oleate into TAG as compared to 49% for mock treated cells showing that the treated cells were functional. As a second test of dietary FA partitioning into lipid rafts, oleate uptake into BB isolated from caveolin-1 gene disrupted mice was greatly reduced (87%) compared to that taken up by BB from WT mice (Fig. 1 A, WT vs. KO). Cholesterol depletion reduced this even further (Fig. 1A, WT-dep vs. KO-dep). The reduced uptake of FA by BB from KO mice was not due to a generalized functional impairment of the BB because of lack of caveolin-1. BB isolated from KO mice were able to take up equivalent amounts of ^{3}H-cholesterol as BB from WT mice (37 ± 3% vs. 36 ± 4% respectively). These data are consistent with the prior data of Valasek [32] who showed that cholesterol uptake by the intestine is not affected by caveolin-1 depletion. The data preliminarily suggested that the oleate taken up by WT BB was dependent on caveolin-1 containing DRM (caveolae).

3.2 Brush border FA distribute into the detergent resistant fraction of an OptiPrep gradient

As a more direct test that the absorbed oleate was in caveolae, we incubated BB with albumin bound ^{3}H-oleate, dissolved the BB in 1% Triton X-100, and then centrifuged the BB on an OptiPrep gradient. On resolution of the gradient, most of the oleate (74%) appeared in the lighter density fractions consistent with DRM (Fig. 1B, closed squares), different than oleate not incubated with BB (Fig. 1B, open rectangles) that distributed to the denser regions of the gradient consistent with the detergent soluble membranes (DSM). By contrast to the oleate incubated with mouse WT BB, when ^{3}H-oleate was incubated with caveolin-1 KO mouse BB (Fig. 1B, open circles), 78% of the oleate distributed to the DSM in the OptiPrep gradient similar to the distribution of oleate not incubated with BB (Fig. 1B, open squares). Caveolin-1, CD36, and IAP, proteins associated with DRM, were all present in the BB-oleate containing fractions as indicated by their immunoblots (Fig. 1C). Importantly, clathrin was not present in the buoyant fractions but was present in the heavy part of the gradient (fraction 9) and in the BB (Fig. 1C). In sum, these data support the thesis that the oleate in BB was in caveolae.

3.3 Caveolin-1 is present in rat and mouse brush border membranes

To confirm caveolin-1 ‘s presence in intestinal BB [33–35], we tested rat and mouse BB for caveolin-1 by immunoblot. We found that caveolin-1 was concentrated in rat BB as compared to whole cell homogenates or cytosol prepared from the homogenates (Fig. 2A). Caveolin-1 was also concentrated in mouse BB compared to cell homogenates (Fig. 2B, lanes 1 and 3) but absent from BB and cell homogenates of caveolin-1 gene disrupted mice (Fig. 2B, lanes 2 and 4). Our anti-caveolin-1 antibody specificity was tested by immunoblotting cytosol that identified 1 band at the Mr of caveolin-1, 22 kDa, (Fig. 2C, lane 1). Prior incubation of the antibody with its immunogenic peptide extinguished the 22 kDa band (Fig. 2C, lane 2) but prior incubation with Sar1b immunogenic peptide did not (Fig. 2C, lane 3). In sum, the data suggest that our anti-caveolin-1 antibody was specific.

3.4 Absorbed cytosolic FA is not bound to FABP1 or 2 but is present in detergent resistant vesicles

Because endocytosis of caveolae from BB is well described [35], we next considered if the BB-oleate was endocytosed and appeared in the cytosol as caveolin-1 containing endocytic vesicles (CEV). If so, this would offer an alternative mechanism to the potential cytosolic FA binder, FABP [36], to sequester cytosolic FA. To differentiate between the 2 potential cytosolic FA-carriers we first used size exclusion chromatography. Cytosol was obtained using the rat intestinal sac model so that only the apical portion of the cell would be exposed to the ^{3}H-oleate. To prevent incorporation of the label into TAG, we pre-incubated the sacs with the acyl-CoA synthetase long chain (ACLS) inhibitor, triacin C [37] and rapidly cooled the sacs post incubation. Despite these precautions, 20% of the absorbed ^{3}H-oleate was incorporated into TAG [5].

We were expecting that the absorbed oleate would be associated with FABP1 or FABP2 [38, 39], small (14 kDa) cytosolic FA binding proteins, or in the FABP1 containing heterotetramer [40] and appear with the smaller proteins. Howener only 5% of the oleate was collected on chromatography of the cytosol over a Sephacryl S-100 HR column. By contrast, of the 2 mg protein put on the column, 1.2 mg was recovered in the eluate suggesting that the oleate dissociated from the majority of the protein. By adjusting the cytosol to 1% Triton X-100 and using 1% Triton X-100 as eluent (Fig. 3A, Sacs) we increased the amount of oleate eluted from the column to 95%. The oleate eluted in 2 peaks; the first peak was at 4 ml suggesting it was in a large structure (Fig. 3A, Sacs). The second peak at 7 ml eluted just before ^{3}H-oleate dissolved in 1% Triton X-100 eluted from the column (8 ml) (Fig. 3 A, Triton X-100) suggesting that the cytosolic oleate was not in Triton X-100 micelles. The requirement for Triton X-100 to elute the oleate and for it to appear in early eluting fractions suggested that the cytosolic oleate was in a detergent resistant fraction. These data are compatible with the thesis that on desorption from the BB, the oleate was in a vesicle, potentially CEV. DRM fractions have been isolated successfully by size exclusion chromatography [29] suggesting that CEV could be similarly isolated.

Since caveolin-1 is known to be present in some DRM and was present in BB, we immunoblotted the column fractions containing oleate for this DRM marker [12]. Caveolin-1 was present in these early eluting fractions as was FAT/CD36, which is also associated with lipid rafts [41] (Fig. 3B). FATP4 [42] and FABP1 were not present in these fractions nor was the lysosomal marker, Rab11. All these proteins were present in intestinal cytosol, however (Fig. 3B, Cyto). The data thus far suggested that the oleate in cytosol was in a large structure, potentially CEV, rather than being bound to FABP.

In order to more clearly separate cytosolic oleate from oleate dissolved in Triton X-100 micelles, we turned to OptiPrep density separation of the cytosol using a method known to

separate DRM from other cellular components [27]. Using this technique, we recovered 57% of the oleate in the low-density fractions (Fig. 4A, fractions 1–3, closed circles) similar to our findings when BB was incubated with oleate (Fig. 1B). Most of the remaining oleate was in the detergent soluble fraction (DSF) toward the heavier part of the gradient (Fig. 4A, fractions 7–9). By contrast to these data, if glyceryltri- ^{3}H-oleate or ^{3}H-oleate were dissolved in 1% Triton X-100 and centrifuged in the OptiPrep gradient, the radioactivity was found in the mid portion (Fig. 4A, fractions 5–6, open squares) or in the denser part of the gradient (Fig. 4A, fractions 7–9, open circles) respectively. We conclude that apically absorbed FA are present in cytosol in a Triton X-100 resistant structure, potentially CEV.

The OptiPrep density fractions were immunoblotted for proteins known to be associated with caveolae. Both caveolin-1 and −2 were identified (Fig. 4B, Fractions 1–2). Caveolin-2 is often associated with caveolin-1 [43] and is required for FA uptake by the intestine in the worm [44]. Surprisingly, caveolin-3, a paralog associated with skeletal and cardiac muscle, was also found in the CEV fraction (Fig. 4B). Like the other caveolins, caveolin-3 is a FA binder [45]. We also immunoblotted for the DRM associated proteins, FAT/CD36 [41] and IAP [46] (Fig. 4B, Fractions 1– 3). Both were found to be present, although they were also present in the denser part of the gradient as well (Fig. 4B, Fractions 7–9). FATP4, FABP1 and FABP2 were all absent from the buoyant fractions(Fig. 4B).

3.5 Absorbed oleate is in caveolin-1 containing vesicles

We took advantage of the caveolin-1 gene disrupted mouse to test the effect of the absence of caveolin-1 in cytosol on the distribution of absorbed cytosolic oleate across the OptiPrep gradient. In WT mice (Fig. 5, WT) absorbed oleate in cytosol is distributed similarly in the OptiPrep gradient to our findings in the rat (Fig. 4A) except that less oleate was in the light fraction (46%) than in the rat (57%). This may be due to less CEV in the mouse than the rat (see below). By contrast, in the caveolin-1 KO mouse, most (79%) of the oleate was in the denser fractions with only 17% in the light fractions (Fig. 5, Cav-KO). These data suggest that caveolin-1 is required to distribute the absorbed oleate into the light OptiPrep fractions consistent with the distribution of CEV.

We next asked what percent of the ^{3}H-oleate in intestinal cytosol was associated with the CEV. To answer this question we immuno-depleted caveolin-1 from cytosol derived from enterocytes absorbing oleate using our rat intestinal sac model. When caveolin-1 immuno-depletion was nearly complete, 91% of the oleate had been removed from the cytosol (Fig. 6A, Caveolin-1). By comparison, similar immunodepletion of caveolin-2 removed only 22% of the oleate (Fig. 6A, Caveolin-2). Although caveolin-1 is thought to be required for caveolin-2 to localize to the apical membrane [47], these two caveolins may be separate [48] as well as having different functional effects [49]. Similarly, 3 rounds of caveolin-3 immunodepletion removed only 17% of the oleate (Fig. 6A, Caveolin-3). These data suggest the possibility that most of the dietary oleate in intestinal cytosol is linked with caveolin-1 associated CEV. The percentage of caveolin-1, caveolin-2, and caveolin-3 remaining in the cytosol after each immunodepletion as judged by immunoblot is shown in Fig. 6B. From 10 to 26% of the caveolins remained after 3 rounds of immunodepletion.

Since FAT/CD36 and IAP were also present in the CEV, we questioned how much oleate could be removed by immuno-depleting these proteins from similarly treated cytosol. However, immuno-depletion of both FAT/CD36 (filled circles) and IAP (filled triangles) only reduced the cytosolic oleate by 55% and 58% respectively (Fig. 6C). Immuno-depletion of similarly treated cytosol using anti-IgG (open squares) and anti-clathrin (open triangles) antibodies reduced cytosolic oleate by 12 and 21% respectively (Fig. 6C). These latter data suggest that the CEV containing the absorbed oleate are not predominantly in clathrin coated endocytotic vesicles in agreement with Fig. 1B.

We next wished to test if the proteins associated with CEV were attached to the vesicle electrostatically or not. To assess this possibility, we compared the distribution of CEV associated proteins in the OptiPrep gradient either before or after adjusting CEV containing cytosol to 2M KC1. When washed with high salt, FAT/CD36 was completely displaced to the more dense fractions indicating its removal from the CEV suggesting that its attachment to the vesicle was by electrostatic forces (Fig. 7A). By comparison, the 2M KC1 wash did not significantly affect the distribution of caveolin-1 or IAP in the gradient (Fig. 7A) as expected [50]. These data suggest that both caveolin-1 and IAP were integrated into the vesicle. The salt wash did not greatly change the oleate distribution in the OptiPrep gradient (Fig. 7B) suggesting that the oleate remained with the CEV, at least in part, under these conditions.

We next questioned if the cytosolic ^{3}H-oleate was present predominantly in the protein or lipid fractions in the cytosol. TCA precipitation of proteins before and after high salt treatment resulted in only 1 ± 0.2% and 2 ± 0.3% of the total oleate present being precipitated respectively. By contrast, if the oleate were bound to albumin, treated or not with high salt, and then precipitated by TCA, 19 ± 2% and 17 ± 3% of the oleate was found in the precipitate respectively. These data suggest that most of the oleate was bound to the lipid portion of CEV rather than the protein component.

Because the proteins present in CEV are associated with lipids or lipid transport, we wished to determine if the proteins were interactive or were merely co-incidentally present in the same column or OptiPrep gradient fractions. To answer this question we performed a series of immuno-precipitations using rat cytosol and antibodies to the 3 known vesicle proteins (Fig. 8). Antibodies against each of the CEV associated proteins, caveolin-1, IAP, and FAT/CD36 were able to co-immuno-precipitate each of the other two as identified by immunoblot. By comparison, antibodies to IgG were unassociated with any of the 3 proteins (data not shown). These data suggest that not only were the proteins found together in the sanjgin vitro fractions but that caveolin-1, FAT/CD36, and IAP were interactive in vivo as well.

We next wished to confirm the presence of CEV in cytosol by visualizing them using negative staining electron microscopy (EM). We used cytosol derived from sacs treated with oleate or not. In the non-oleate exposed cytosols, a large number of rounded, vesicular appearing structures of varying size were seen (Fig. 9A) which averaged 57.4 24 nm diameter (1 SD of 227 vesicles counted). Vesicles in cytosol from oleate-exposed enterocytes were of similar but more uniform size (av. diameter 55.4 3.0 nm [1 SD of 250 vesicles counted]) (Fig. 9B). By contrast, the number of vesicles per photograph at 20,000 X magnification on oleate feeding was significantly greater than found in the absence of oleate (44 ± 6.2 vs. 14 ± 3, $p < 0.001$ vesicles per portion of the grid examined, 15 and 7 grids examined respectively).

To clarify if the vesicles seen in Fig. 9A and 9B contained caveolin-1, we employed immuno-EM using anti-caveolin-1 antibodies. The antibody identified many labeled vesicles in cytosol derived from cells not exposed to oleate (Fig. 10A, compare with IgG antibody, Fig. 10B) and from cells exposed to oleate (Fig. 10C, compare with IgG antibody, Fig. 10D).

3.17 To confirm the role of caveolin-1 in CEV formation, we turned to the caveolin-1 knock out mouse. In the WT mouse, we found that the vesicle size in the cytosol of enterocytes derived from non-oleate fed cells was the same as the rat (av. 60.7 ± 25 nm in diameter, 63 vesicles examined) and, similar to the rat, the size of the vesicles was unchanged in response to exposure to oleate (av. 57.4 ± 23 nm in diameter, 182 vesicles examined). Also similar to

the rat, the number of vesicles per 20,000 X photograph was greatly increased on oleate feeding (3 ± 1.5 vs. 14 ± 2.9, $p < 0.027$). Electron microscopic images of the vesicles from non-oleate fed and oleate fed WT intestinal sac enterocyte cytosol are shown in Fig. 11A and B respectively). By contrast, in the caveolin-1 KO mouse, no vesicles were seen irrespective of oleate feeding (Fig. 11 C and D respectively).

3.6 Caveolin-1 KO mice have an impaired uptake of FA by the intestine, a reduced weight gain, and more steatorrhea on a high fat diet than do WT mice

The total data would suggest that the caveolin-1 KO mouse would have a reduced ability to absorb dietary FA as compared to WT mice. To test this possibility, we gavaged 0.2 ml corn oil supplemented with ^{3}H-oleate into WT and KO mice. 30 min post gavage we harvested the stomach, intestinal contents, the intestine, and cecum from each mouse. Analysis of the gastric contents showed that an equivalent ($p = 0.28$) amount of corn oil-oleate left the stomach after 30 min. (Fig. 12A, stomach). By contrast, 4.5 fold more oleate was found in the intestinal lumen of the KO mice vs. the WT mice suggesting impaired uptake of the oleate presented to the intestine for absorption in the KO mice (Fig. 12A, Lumen). Equivalent amounts of oleate remained in the intestine of both genotypes (Fig. 12A, intestine). Consistent with the intestinal luminal data, more oleate was present in the cecal contents of the KO mice as compared to the WT mice (Fig. 12A, cecum) although the amount of oleate present was small due to the short time period of observation.

Consistent with these data, on a high fat diet (23%, w:w), caveolin-1 KO mice had a reduced weight gain compared to WT controls (data not shown) in agreement with the work of Razani et al. [12]. By contrast, mice of either genotype fed the chow diet (4% fat diet) gained equal amounts of weight. Finally, we next questioned if the reduced weight gain in the KO mice on the high fat diet as compared to the WT mice were due to their impaired ability to absorb dietary fat as suggested in Fig. 12A. To test this potential, we measured the fat in the stool of both the WT and KO mice on the chow and the fat supplemented diet. On the chow diet, the WT and KO mice both excreted 8 mg of fat per day in their stool (Fig. 12B). On the fat supplemented diet, the WT mice had 14 mg fat in their stool, a significant increase over the chow diet. However, the KO mice on the high fat diet had double the amount of fat in their stool (28 mg) as the WT mice (Fig. 12B). These data suggest that the excess steatorrhea found in the KO mice vs. the WT mice contributed to their reduced weight gain. The differences in fat excretion between the WT and KO mice cannot be explained on the basis of a differential intake of diet, each of 2 WT mice ate 42 g food in 2 weeks and each of 2 KO mice ate 38 g food in two weeks. Because we measured total stool lipid and not specifically triacylglycerols as did Razani et al. [12], we were able to show a difference in stool lipids between genotypes on the high fat diet. This is because most stool lipid is present as FA [51] as was the case here (98% of the stool fat was FA when the stool fats were separated by thin layer chromatography). Further, our results may have been influenced by the amount of milk fat used in our high fat diet (21% of 23% (w:w) dietary fat was milk fat). Since the sn-3 position of milk fat is C1O and is water soluble, we may have overestimated the ability of the KO mice to absorb dietary fat.

4. DISCUSSION

The results of this study support the thesis that the mechanism by which enterocytes absorb dietary FA is by associating with BB caveolae. The data further suggest that the FA containing CEV are endocytic products of BB caveolae and potentially deliver their FA cargo directly to the ER (not shown here). This thesis is supported by our findings that both the DRM of BB and CEV concentrate absorbed oleate, contain proteins associated with lipid rafts (caveolin-1, FAT/CD36, IAP), and exclude clathrin suggesting that the CEV are derived from BB. Using CEV as cytosolic dietary FA carriers could enable the transport of

large amounts of FA from the apical membrane to the ER in a controlled environment avoiding the known membrane disruptive effects of FA [1].

The amount of caveolin in intestinal BB is controversial. Some investigators have found little [33, 52] whereas others have found it to be present in abundant amounts [8 secretory vesicles, cytoplasm or mitochondria, 34, 35]. Our data support the presence of caveolin-1 in BB both by immunoblot and by experiments using caveolin-1 gene disrupted mice that suggested a functional role for caveolin-1 in BB. The caveolin-1 KO mice were not able to take up as much FA into their intestinal BB, on a high fat diet not able to gain as much weight and had more steatorrhea in comparison to WT mice.

Once FA are absorbed, there is considerable both direct and indirect evidence that FABP1 and FABP2 function to transport FA within enterocytes as summarized by Storch [36, 53]. In support of this thesis, FABP2 has been shown to redistribute from the apical membrane to the cytosol in response to fat feeding [54]. However, the amount of absorbed FA bound to FABP1 and FABP2 was found to be only 10 fmol and 2 fmol/mg cytosolic protein respectively [54]. By contrast, in our rat enterocytes the FA concentration measured by the specific activity of the ^{3}H-oleate was 1.6 μmol/mg cytosolic protein. The actual oleate concentration is likely to be twice as much due to dilution of the radiolabel with endogenous FA [55]. These data should also be compared to the FABP concentration in intestinal cytosol (2.9 nmol/mg cytosolic protein, FABP1 + FABP2) [4]. Since FABP1 can only bind 2 mol FA per mol of FABP1 and FABP2 can bind 1 mol of FA per mol FABP2 [53], it is evident that most of the absorbed FA in intestinal cytosol is not bound to either FABP. These data suggest that other binding mechanisms might exist in intestinal cytosol. The accuracy of our FA data may be somewhat reduced by the fact that some of the FA could have partitioned into cellular membranes and/or solubilized in the Triton X-100.

Important for the current report, caveolin-1 is localized to the cytosolic side of the apical membrane [45, 50] where it associates with the lipid components of the raft, cholesterol and sphingomyelin. In addition, the C terminus contains multiple positively charged amino acid residues to which FA could potentially bind. However, TCA precipitation of 1% Triton X-100 solubilized BB contained only 1–2% of the total BB oleate implying that most of the oleate was associated with the lipid components of the caveolae.

Although it is well recognized that caveolin-1 is associated with FA binding at the cell surface of multiple cell types [9–11] including the intestine [34] and specifically human intestine [33, 34], to our knowledge this is the first study to suggest that most of the absorbed dietary FA remain associated with caveolin-1 containing CEV in the cytosol although others have suggested that some may be present [20]. The endocytic vesicles described by Danielsen's group contain not only IAP as we confirm here, but also clathrin [56]. We were unable to identify clathrin either in the oleate containing Triton X-100 resistant portion of the BB or in CEV, findings supported by studies showing the absence of clathrin in caveolae [57–59].

In support of the thesis that caveolae promote FA absorption in cells, the expression of caveolin-1 [10] or caveolin-3 [45] in HEK293 cells both stimulate entry of FA into the cells and in the case of caveolin-3 results in increased TAG synthesis. These data parallel the pathway suggested for cholesterol absorption across the apical membrane and delivery to the ER [34]. In both studies, however, the mechanism by which cholesterol is transported in the cytosol was not directly addressed. Our proposed model for absorbed FA transit through the cytosol may also be relevant to cholesterol and operative in other cell types such as the adipocyte where large amounts of FA flux through the surface membrane [14, 60].

In further support of the thesis that caveolae provide the absorptive surface for dietary FA rather than specific transport proteins, intestinal cells exposed to FA in bile salt micelles show increased FA in the apical membrane as compared to other cell constituents [56]. Pulse chase studies using BODIPY labeled FA confirm these findings [20]. Taken together, the data suggest that the absorbed FA accumulate in an FA interactive environment rather than being specifically bound to transport proteins that could only provide small amounts of FA binding on a molar basis. This thesis is supported by data in HEK293 cells in which CD36 and FATP4 were shown not to participate in FA uptake across the cellular membrane whereas caveolin-1 did [10]. In addition, the increased FA suggested to be in BB-caveolae potentiate the endocytosis of the caveolae [61] providing a mechanism for increasing CEV in the cytosol in response to lipid feeding as shown here.

Our data are not necessarily in conflict with those of Chow and Hollander [62] who proposed simple or facilitated diffusion of FA depending on the FA concentration because the kinetics of the flux of FA into caveolae could appear compatible with either interpretation. Further, the saturation kinetics proposed by Murota and Storch to indicate protein mediated absorption [63] could be the result of only a certain amount of FA able to be absorbed by the caveolae.

By contrast to the data in caveolin-1 KO mice showing reduced FA absorption, cholesterol absorption is not affected in the same genetically modified mice [32]. Further, caveolin-1 KO mice are fully sensitive to ezetimibe, an inhibitor of NPC1L1, the protein associated with cholesterol absorption. In addition, NPC1L1 is endocytosed via a clathrin associated mechanism [64]. As we show here, CEV do not contain clathrin. Finally, cholesterol is taken up by the BB of the caveolin-1 KO mice at a rate similar to its uptake in WT mice BB. The total data suggest that the pathways of cholesterol and FA absorption from the apical membrane are different.

FAT/CD36 is a transmembrane protein [65] whose transport to the apical membrane of intestinal cells requires caveolin-1 [11]. However, CD36 may not be integrated into endocytosed caveolae in cytosol in a manner similar to its orientation in membranes. This suggestion is supported by our data showing that high salt treatment redistributes CD36 from CEV to the denser regions an OptiPrep gradient, in contrast to caveolin-1 and IAP that remain with the more buoyant fractions.

IAP has long been known to be associated with lipid absorption [21] but more recent data has suggested otherwise [22, 23]. Our data show that IAP is interactive with caveolin-1, as well as FAT/CD36, and like caveolin-1, is not displaced from the light to the denser portions of the OptiPrep gradient by high salt suggesting its robust integration into CEV.

By contrast to the caveolin-1, CD36, and IAP data, immunodepletion of clathrin from the cytosol does not affect the cytosolic oleate content. These data are consistent with the fact that endocytosed clathrin coated pits are in separate vesicles from endocytosed caveolae [66].

Our data are consistent with the hypothesis that most absorbed dietary FA are associated with caveolae in the apical membrane and remain with caveolin-1 associated CEV on endocytosis. The CEV-FA offers a pathway keeping dietary FA in a physico-chemically inert structure so that the FA do not disrupt cellular membranes prior to their incorporation into TAG in the ER. This thesis is also consistent with the pinocytotic pathway of lipid absorption suggested by Palay and Karlin [67]. Although it is attractive to consider that the CEV have a targeting mechanism to the ER, our data do not directly address this issue but are consistent with this thesis. Current work in our laboratory is directed at testing this model.

Acknowledgments

The authors would like to acknowledge helpful discussions with Shadab A. Siddiqi, Ph. D. regarding this work. This study was supported by National Institute of Diabetes and Digestive and Kidney Diseases (NIDDK) of the National Institutes of Health Grant [DK-074565] (C.M.M.), a Veterans Administration Merit Award (CMM), and NIH Medical Student Research Program Grant [T35DK07405] (A.S. and M. B.).

References

1. Listenberger LL, Han X, Lewis SE, Cases S, Farese RV Jr. Ory DS, Schaffer JE. Triglyceride accumulation protects against fatty acid-induced lipotoxicity. Proc Natl Acad Sci U S A. 2003; 100:3077–3082. [PubMed: 12629214]
2. Mansbach CM 2nd, Cohen RS, Leff PB. Isolation and properties of the mixed lipid micelles present in intestinal content during fat digestion in man. J Clin Invest. 1975; 56:781–791. [PubMed: 1159087]
3. Black PN, DiRusso CC. Isolation and properties of the mixed lipid micelles present in intestinal content during fat digestion in man. Microbiol Mol Biol Rev. 2003; 67:454–472. table of contents. [PubMed: 12966144]
4. Bass NA, Manning JA, Ockner RK, Gordon JI, Seetharam S, Alpers DH. Regulation of the biosynthesis of two distinct fatty acid-binding proteins in rat liver and intestine. J Biol Chem. 1985; 260:1432–1436. [PubMed: 3968078]
5. Mansbach CM 2nd, Nevin P. Intracellular movement of triacylglycerols in the intestine. J Lipid Res. 1998; 39:963–968. [PubMed: 9610762]
6. Pike LJ. Rafts defined: a report on the Keystone Symposium on Lipid Rafts and Cell Function. J Lipid Res. 2006; 47:1597–1598. [PubMed: 16645198]
7. Kunding AH, Christensen SM, Danielsen EM, Hansen GH. Domains of increased thickness in microvillar membranes of the small intestinal enterocyte. Mol Membr Biol. 2010; 27:170–177. [PubMed: 20540667]
8. Li WP, Liu P, Pilcher BK, Anderson RG. Cell-specific targeting of caveolin-1 to caveolae, secretory vesicles, cytoplasm or mitochondria. J Cell Sci. 2001; 114:1397–1408. [PubMed: 11257005]
9. Trigatti BL, Anderson RG, Gerber GE. Identification of caveolin-1 as a fatty acid binding protein. Biochem Biophys Res Commun. 1999; 255:34–39. [PubMed: 10082651]
10. Meshulam T, Simard JR, Wharton J, Hamilton JA, Pilch PF. Role of caveolin-1 and cholesterol in transmembrane fatty acid movement. Biochemistry. 2006; 45:2882–2893. [PubMed: 16503643]
11. Ring A, Le Lay S, Pohl J, Verkade P, Stremmel W. Caveolin-1 is required for fatty acid tramljocase (FAT/CD36) localization and function at the plasma membrane of mouse embryonic fibroblasts. Biochim Biophys Acta. 2006; 1761:416–423. [PubMed: 16702023]
12. Razani B, Combs TP, Wang XB, Frank PG, Park DS, Russell RG, Li M, Tang B, Jelicks LA, Scherer PE, Lisanti MP. Caveolin-1-deficient mice are lean, resistant to diet-induced obesity, and show hypertriglyceridemia with adipocyte abnormalities. J Biol Chem. 2002; 277:8635–8647. [PubMed: 11739396]
13. Pike LJ. Lipid rafts: bringing order to chaos. J Lipid Res. 2003; 44:655–667. [PubMed: 12562849]
14. Pohl J, Ring A, Korkmaz U, Ehehalt R, Stremmel W. FAT/CD36-mediated long-chain fatty acid uptake in adipocytes requires plasma membrane rafts. Mol Biol Cell. 2005; 16:24–31. [PubMed: 15496455]
15. Harmon CM, Luce P, Beth AH, Abumrad NA. Labeling of adipocyte membranes by sulfo-N-succinimidyl derivatives of long-chain fatty acids: inhibition of fatty acid transport. J Membr Biol. 1991; 121:261–268. [PubMed: 1865490]
16. Nassir F, Wilson B, Han X, Gross RW, Abumrad NA. CD36 is important for fatty acid and cholesterol uptake by the proximal but not distal intestine. J Biol Chem. 2007; 282:19493–19501. [PubMed: 17507371]
17. Nauli AM, Nassir F, Zheng S, Yang Q, Lo CM, Vonlehmden SB, Lee D, Jandacek RJ, Abumrad NA, Tso P. CD36 is important for chylomicron formation and secretion and may mediate cholesterol uptake in the proximal intestine. Gastroenterology. 2006; 131:1197–1207. [PubMed: 17030189]

18. Goudriaan JR, Dahlmans VE, Febbraio M, Teusink B, Romijn JA, Havekes LM, Voshol PJ. Intestinal lipid absorption is not affected in CD36 deficient mice. Mol Cell Biochem. 2002; 239:199–202. [PubMed: 12479586]
19. Schroeder R, London E, Brown D. Interactions between saturated acyl chains confer detergent resistance on lipids and glycosylphosphatidylinositol (GPI)-anchored proteins: GPI-anchored proteins in liposomes and cells show similar behavior. Proc Natl Acad Sci U S A. 1994; 91:12130–12134. [PubMed: 7991596]
20. Hansen GH, Rasmussen K, Niels-Christiansen LL, Danielsen EM. Dietary free fatty acids form alkaline phosphatase-enriched microdomains in the intestinal brush border membrane. Molecular membrane biology. 2011; 28:136–144. [PubMed: 21166483]
21. Glickman RM, Alpers DH, Drummey GD, Isselbacher KJ. Increased lymph alkaline phosphatase after fat feeding: effects of medium chain triglycerides and inhibition of protein synthesis. Biochim Biophys Acta. 1970; 201:226–235. [PubMed: 5418723]
22. Nauli AM, Zheng S, Yang Q, Li R, Jandacek R, Tso P. Intestinal alkaline phosphatase release is not associated with chylomicron formation. Am J Physiol Gastrointest Liver Physiol. 2003; 284:G583–G587. [PubMed: 12466148]
23. Nakano T, Inoue I, Koyama I, Kanazawa K, Nakamura K, Narisawa S, Tanaka K, Akita M, Masuyama T, Seo M, Hokari S, Katayama S, Alpers DH, Millan JL, Komoda T. Disruption of the murine intestinal alkaline phosphatase gene Akp3 impairs lipid transcytosis and induces visceral fat accumulation and hepatic steatosis. Am J Physiol Gastrointest Liver Physiol. 2007; 292:G1439–G1449. [PubMed: 17332477]
24. Siddiqi SA, Gorelick FS, Mahan JT, Mansbach CM 2nd. COPII proteins are required for Golgi fusion but not for endoplasmic reticulum budding of the pre-chylomicron transport vesicle. J Cell Sci. 2003; 116:415–427. [PubMed: 12482926]
25. Weiser M. Intestinal epithelial cell surface membrane glycoprotein synthesis: I. An indicator of cellular differentiation. J Biol Chem. 1973; 248:2536–2541. [PubMed: 4698230]
26. Kessler M, Acuto O, Storelli C, Murer H, Muller M, Semenza G. A modified procedure for the rapid preparation of efficiently transporting vesicles from small intestinal brush border membranes. Their use in investigating some properties of D-glucose and choline transport systems. Biochimica et biophysica acta. 1978; 506:136–154. [PubMed: 620021]
27. Harder T, Scheiffele P, Verkade P, Simons K. Lipid domain structure of the plasma membrane revealed by patching of membrane components. J Cell Biol. 1998; 141:929–942. [PubMed: 9585412]
28. Danthi P, Chow M. Cholesterol removal by methyl-beta-cyclodextrin inhibits poliovirus entry. J Virol. 2004; 78:33–41. [PubMed: 14671085]
29. Radeva G, Sharom FJ. Isolation and characterization of lipid rafts with different properties from RBL-2H3 (rat basophilic leukaemia) cells. Biochem J. 2004; 380:219–230. [PubMed: 14769131]
30. Folch J, Lees M, Sloan-Stanley GH. A simple method for the isolation and purification of total lipids from animal tissues. J. Biol. Chem. 1957; 226:497–509. [PubMed: 13428781]
31. Schwarz M, Lund EG, Setchell KD, Kayden HJ, Zerwekh JE, Bjorkhem I, Herz J, Russell DW. Disruption of cholesterol 7alpha-hydroxylase gene in mice. II. Bile acid deficiency is overcome by induction of oxysterol 7alpha-hydroxylase. The Journal of biological chemistry. 1996; 271:18024–18031. [PubMed: 8663430]
32. Valasek MA, Weng J, Shaul PW, Anderson RG, Repa JJ. Caveolin-1 is not required for murine intestinal cholesterol transport. J Biol Chem. 2005; 280:28103–28109. [PubMed: 15919660]
33. Badizadegan K, Dickinson BL, Wheeler HE, BluWteg RS, Holmes RK, Lencer WI. Heterogeneity of detergent-insoluble membranes from human intestine containing caveolin-1 and ganglioside G(M1). Am J Physiol Gastrointest Liver Physiol. 2000; 278:G895–G904. [PubMed: 10859219]
34. Field FJ, Born E, Murthy S, Mathur SN. Caveolin is present in intestinal cells: role in cholesterol trafficking? J Lipid Res. 1998; 39:1938–1950. [PubMed: 9788240]
35. Hansen GH, Niels-Christiansen LL, Immerdal L, Danielsen EM. Scavenger receptor class B type I (SR-BI) in pig enterocytes: trafficking from the brush border to lipid droplets during fat absorption. Gut. 2003; 52:1424–1431. [PubMed: 12970134]

36. Storch J, Corsico B. The Emerging Functions and Mechanisms of Mammalian Fatty Acid-Binding Proteins. Annu Rev Nutr. 2008
37. Igal RA, Wang P, Coleman RA. Triacsin C blocks de novo synthesis of glycerolipids and cholesterol esters but not recycling of fatty acid into phospholipid: evidence for functionally separate pools of acyl-CoA. Biochem J. 1997; 324(Pt 2):529–534. [PubMed: 9182714]
38. Falomir-Lockhart LJ, Franchini GR, Guerbi MX, Storch J, Corsico B. Interaction of enterocyte FABPs with phospholipid membranes: clues for specific physiological roles. Biochimica et biophysica acta. 2011; 1811:452–459. [PubMed: 21539932]
39. Glatz JF, Storch J. Unravelling the significance of cellular fatty acid-binding proteins. Curr Opin Lipidol. 2001; 12:267–274. [PubMed: 11353329]
40. Siddiqi S, Mansbach CM 2nd. Phosphorylation of Sarlb protein releases liver fatty acid-bindingplotein from multiprotein complex in intestinal cytosol enabling it to bind to endoplasmic reticulum (ER) and bud the pre-chylomicron transport vesicle. J Biol Chem. 2012; 287:10178–10188. [PubMed: 22303004]
41. Ehehalt R, Sparla R, Kulaksiz H, Herrmann T, Fullekrug J, Stremmel W. Uptake of long chain fatty acids is regulated by dynamic interaction of FAT/CD36 with cholesterol/sphingolipid enriched microdomains (lipid rafts). BMC Cell Biol. 2008; 9:45. [PubMed: 18700980]
42. Stahl A, Hirsch DJ, Gimeno RE, Punreddy S, Ge P, Watson N, Patel S, Kotler M, Raimondi A, Tartaglia LA, Lodish HF. Identification of the major intestinal fatty acid transport protein. Mol Cell. 1999; 4:299–308. [PubMed: 10518211]
43. Scherer PE, Lewis RY, Volonte D, Engelman JA, Galbiati F, Couet J, Kohtz DS, van Donselaar E, Peters P, Lisanti MP. Cell-type and tissue-specific expression of caveolin-2. Caveolins 1 and 2 co-localize and form a stable hetero-oligomeric complex in vivo. J Biol Chem. 1997; 272:29337–29346. [PubMed: 9361015]
44. Parker S, Walker DS, Ly S, Baylis HA. Caveolin-2 is required for apical lipid trafficking and suppresses basolateral recycling defects in the intestine of Caenorhabditis elegans. Mol Biol Cell. 2009; 20:1763–1771. [PubMed: 19158391]
45. Simard JR, Meshulam T, Pillai BK, Kirber MT, Brunaldi K, Xu S, Pilch PF, Hamilton JA. Caveolins sequester FA on the cytoplasmic leaflet of the plasma membrane, augment triglyceride formation, and protect cells from lipotoxicity. J Lipid Res. 2010; 51:914–922. [PubMed: 20388923]
46. Danielsen EM. Involvement of detergent-insoluble complexes in the intracellular transport of intestinal brush border enzymes. Biochemistry. 1995; 34:1596–1605. [PubMed: 7849019]
47. Williams TM, Lisanti MP. The caveolin proteins. Genome Biol. 2004; 5:214. [PubMed: 15003112]
48. Oikawa E, Iijima H, Suzuki T, Sasano H, Sato H, Kamataki A, Nagura H, Kang MJ, Fujino T, Suzuki H, Yamamoto TT. A novel acyl-CoA synthetase, ACS5, expressed in intestinal epithelial cells and proliferating preadipocytes. J Biochem. 1998; 124:679–685. [PubMed: 9722683]
49. Song KS, Scherer PE, Tang Z, Okamoto T, Li S, Chafel M, Chu C, Kohtz DS, Lisanti MP. Expression of caveolin-3 in skeletal, cardiac, and smooth muscle cells. Caveolin-3 is a component of the sarcolemma and co-fractionates with dystrophin and dystrophin-associated glycoproteins. J Biol Chem. 1996; 271:15160–15165. [PubMed: 8663016]
50. Dietzen DJ, Hastings WR, Lublin DM. Caveolin is palmitoylated on multiple cysteine residues. Palmitoylation is not necessary for localization of caveolin to caveolae. J Biol Chem. 1995; 270:6838–6842. [PubMed: 7896831]
51. Van De Kamer JH. Quantitative determination of the saturated and unsaturated higher fatty acids in fecal fat. Scandinavian journal of clinical and laboratory investigation. 1953; 5:30–36. [PubMed: 13064609]
52. Mirre C, Monlauzeur L, Garcia M, Delgrossi MH, Le Bivic A. Detergent-resistant membrane microdomains from Caco-2 cells do not contain caveolin. The American journal of physiology. 1996; 271:C887–C894. [PubMed: 8843719]
53. Storch J, Thumser AE. The fatty acid transport function of fatty acid-binding proteins. Biochim Biophys Acta. 2000; 1486:28–44. [PubMed: 10856711]

54. Alpers DH, Bass NM, Engle MJ, DeSchryver-Kecskemeti K. Intestinal fatty acid binding protein may favor differential apical fatty acid binding in the intestine. Biochim Biophys Acta. 2000; 1483:352–362. [PubMed: 10666570]
55. Mansbach CM II, Partharsarathy S. A re-examination of the fate of glyceride glycerol in neutral lipid absorption and transport. J. Lipid Res. 1982; 23:1009–1019. [PubMed: 7142810]
56. Hansen GH, Niels-Christiansen LL, Immerdal L, Nystrom BT, Danielsen EM. Intestinal alkaline phosphatase: selective endocytosis from the enterocyte brush border during fat absorption. Am J Physiol Gastrointest Liver Physiol. 2007; 293:G1325–G1332. [PubMed: 17947448]
57. Doherty GJ, McMahon HT. Mechanisms of endocytosis. Annual review of biochemistry. 2009; 78:857–902.
58. Kirkham M, Parton RG. Clathrin-independent endocytosis: new insights into caveolae and non-caveolar lipid raft carriers. Biochim Biophys Acta. 2005; 1746:349–363. [PubMed: 16440447]
59. Parton RG, Simons K. The multiple faces of caveolae. Nat Rev Mol Cell Biol. 2007; 8:185–194. [PubMed: 17318224]
60. Pohl J, Ring A, Ehehalt R, Schulze-Bergkamen H, Schad A, Verkade P, Stremmel W. Long-chain fatty acid uptake into adipocytes depends on lipid raft function. Biochemistry. 2004; 43:4179–4187. [PubMed: 15065861]
61. Lipowsky R. Domain-induced budding of fluid membranes. Biophys J. 1993; 64:1133–1138. [PubMed: 19431884]
62. Chow SL, Hollander D. Linoleic acid absorption in the unanesthetized rat: mechanism of transport and influence of luminal factors on absorption. Lipids. 1979; 14:378–385. [PubMed: 35725]
63. Murota K, Storch J. Uptake of micellar long-chain fatty acid and sn-2-monoacylglycerol into human intestinal Caco-2 cells exhibits characteristics of protein-mediated transport. J Nutr, Jul. 2005; 135(7):1626–1630.
64. Ge L, Wang J, Qi W, Miao HH, Cao J, Qu YX, Li BL, Song BL. The cholesterol absorption inhibitor ezetimibe acts by blocking the sterol-induced internalization of NPC1L1. Cell metabolism. 2008; 7:508–519. [PubMed: 18522832]
65. Tao N, Wagner SJ, Lublin DM. CD36 is palmitoylated on both N- and C-terminal cytoplasmic tails. J Biol Chem. 1996; 271:22315–22320. [PubMed: 8798390]
66. Le PU, Nabi IR. Distinct caveolae-mediated endocytic pathways target the Golgi apparatus and the endoplasmic reticulum. J Cell Sci. 2003; 1l6:1059–1071. [PubMed: 12584249]
67. Palay SL, Karlin LJ. An electron microscopic study of the intestinal villus. II. The pathway of fat absorption. The Journal of biophysical and biochemical cytology. 1959; 5:373–384. [PubMed: 13664677]

Highlights

1. Caveolin-1 knock out mouse apical brush border membranes do not take up oleate.
2. Absorbed oleate is in detergent resistant fractions in intestinal apical brush borders.
3. 91% of absorbed oleate in intestinal cytosol is in caveolin-1 containing vesicles.
4. No cytosolic oleate containing vesicles are found in caveolin-1 knock out cytosol.
5. Caveolin-1 knock out mice have a reduced weight gain and more stool fat.

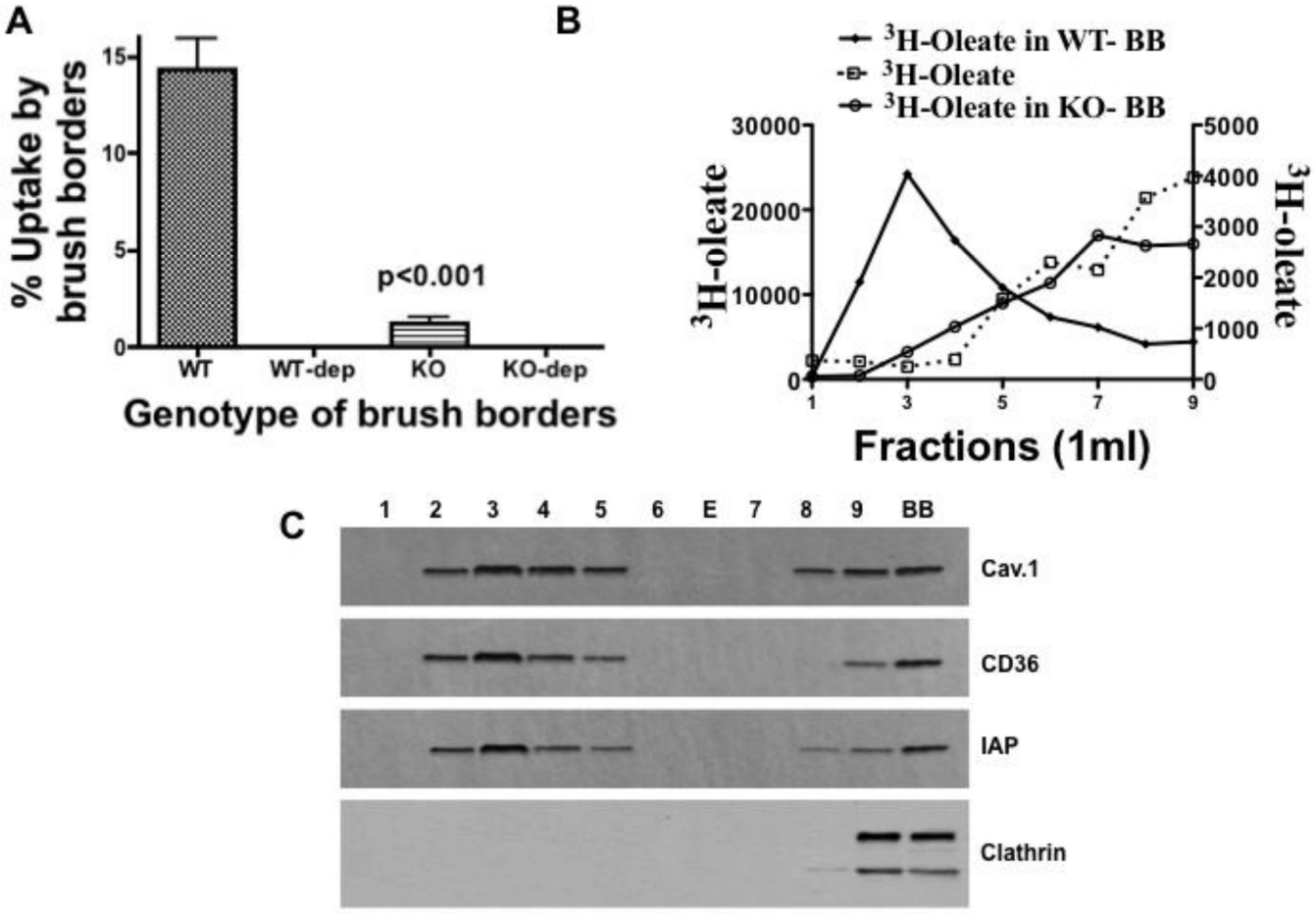

Fig. 1.

Oleate uptake by intestinal brush border membranes is caveolin-1 dependent and is in detergent resistant membranes. A. BB from WT (WT) and KO (KO) mice were prepared and incubated with ^{3}H-oleate bound to albumin (Methods). The percentage of ^{3}H-oleate taken up by both sets of BB is shown on the ordinate. The BB from both mouse genotypes were depleted of cholesterol (WT-dep) and (KO-dep) (Methods) and tested for albumin bound ^{3}H-oleate uptake. The percentage of ^{3}H-oleate taken up by both BB preparations is shown on the ordinate. The data are the mean ± SEM (N = 4). The p value tests the differences between the means of the native WT and KO BB preparations. B. The distribution of oleate in an OptiPrep gradient when incubated with (WT or KO) BB or without BB. ^{3}H-oleate was incubated either with 1 mg prot WT-BB (closed squares), KO-BB (open circles), or by itself (open squares) at 37°C for 30 min. The brush borders were washed twice, re-isolated by centrifugation, and dissolved in 1% Triton X-100. The resulting mixture was placed at the bottom of an OptiPrep gradient and centrifuged for 20h (Methods). The gradient was resolved, 1 ml fractions collected (9 ml total volume), and the total ^{3}H-oleate-dpm determined. C. Immunoblots (50 (μg prot) for caveolin-1, CD36, intestinal alkaline phosphatase (IAP), and clathrin are shown for each OptiPrep fraction. BB is the brush border fraction. E is empty lane.

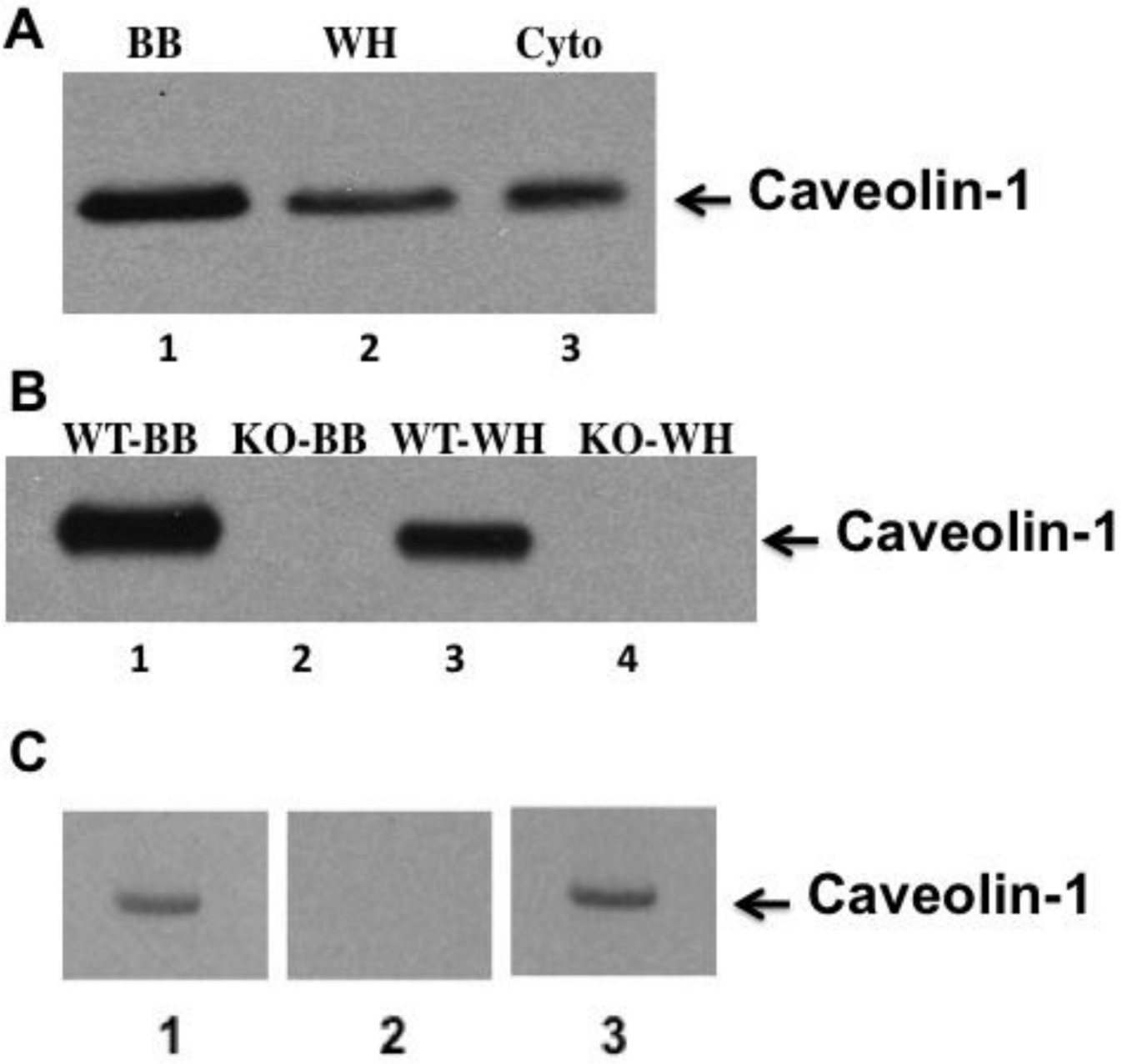

Fig. 2.

Caveolin-1 is expressed in the BB of rat and WT mouse intestinal cells but absent in caveolin-1 KO mice. A. An immunoblot using anti-caveolin-1 antibody was performed on rat intestinal BB, whole cell homogenate, and cytosol separated by SDS-PAGE (35 μg prot). Lane 1 is BB (BB), lane 2 is whole cell homogenate (WH), and lane 3 is cytosol (Cyto). B. Immunoblots using caveolin-1 antibodies were performed using 35 (μg protein separated by SDS-PAGE of mouse BB from WT mice (WT-BB) (Lane 1), caveolin-1 KO mice (KO-BB) (Lane 2) and whole cell homogenates from WT mice (WT-WH) (Lane 3) and caveolin-1 KO mice (KO-WH) (Lane 4). C. Rat cytosol (30 μg) immunoblotted using anti-caveolin-1 antibodies (Lane 1), anti-caveolin-1 antibodies pre-treated with caveolin-1 immunogenic peptide (Lane 2), anti-caveolin-1 antibodies pretreated with Sarlb immunogenic peptide

(Lane 3). The protocol provided by Santa Cruz Biotechology was used for the addition of the peptides. Immunoblots were detected by ECL.

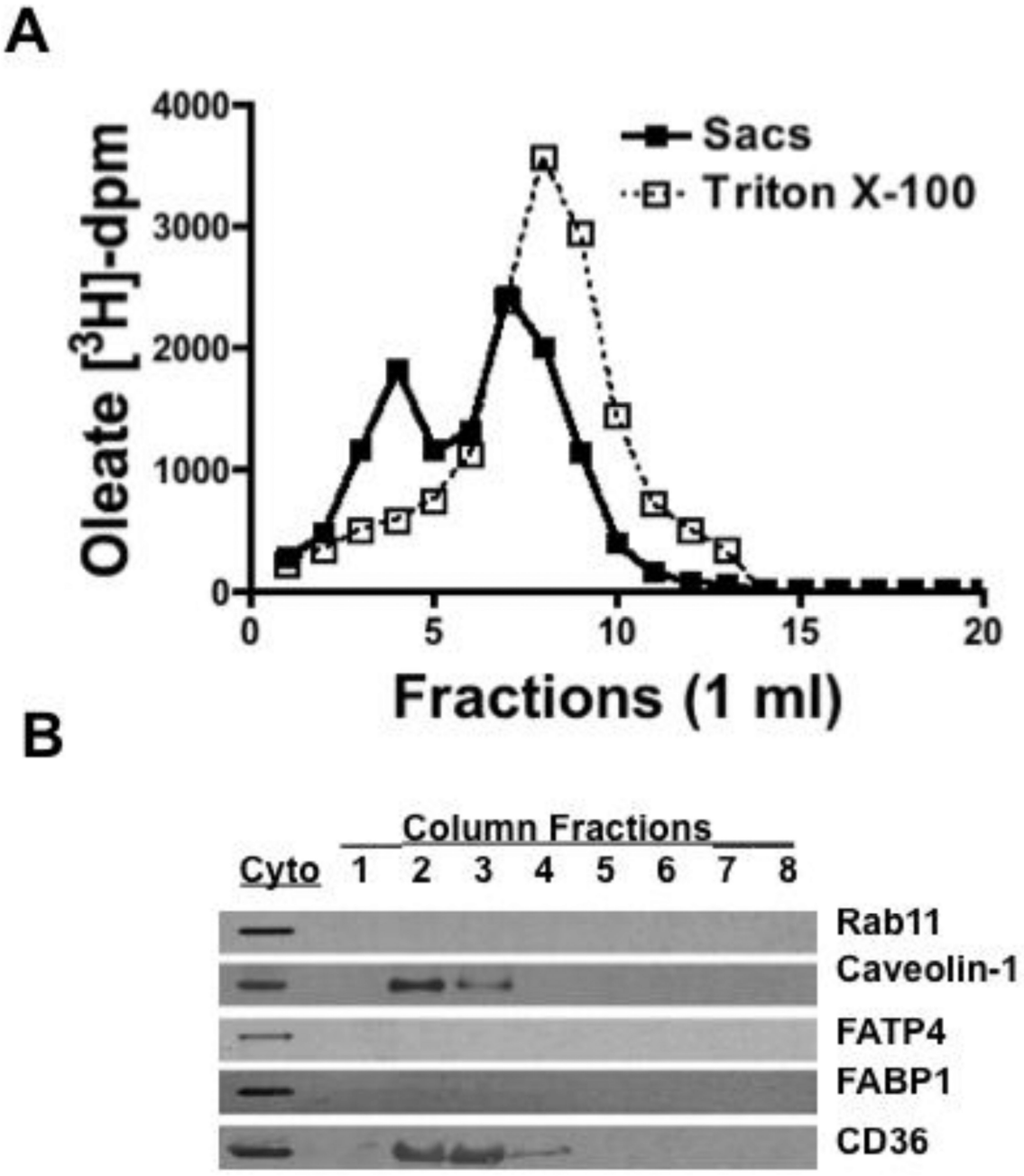

Fig. 3.

A. Cytosol derived from enterocytes from rat intestinal sacs exposed to ^{3}H-oleate (Sacs, closed squares) or ^{3}H-oleate alone (open squares) were treated withl% Triton X-100 and chromatographed over a Sephacryl S-100 HR column equilibrated with Triton X-100. Fractions of 1 ml were collected from the column and oleate-dpm determined. B. Below the graph is shown immunoblots (50 (μg prot) for Rabl 1, caveolin-1, FATP4, FABP1, and CD36 from fractions 1 to 8 (fraction 8 is a combination of fractions 8 to 11) as indicated to the right of the blots. Immunoblots for each protein in native cytosol was also performed (Cyto). FABP1 and rab11 appeared in fractions 15– 18 (not shown). The data are representative of 3 trials.

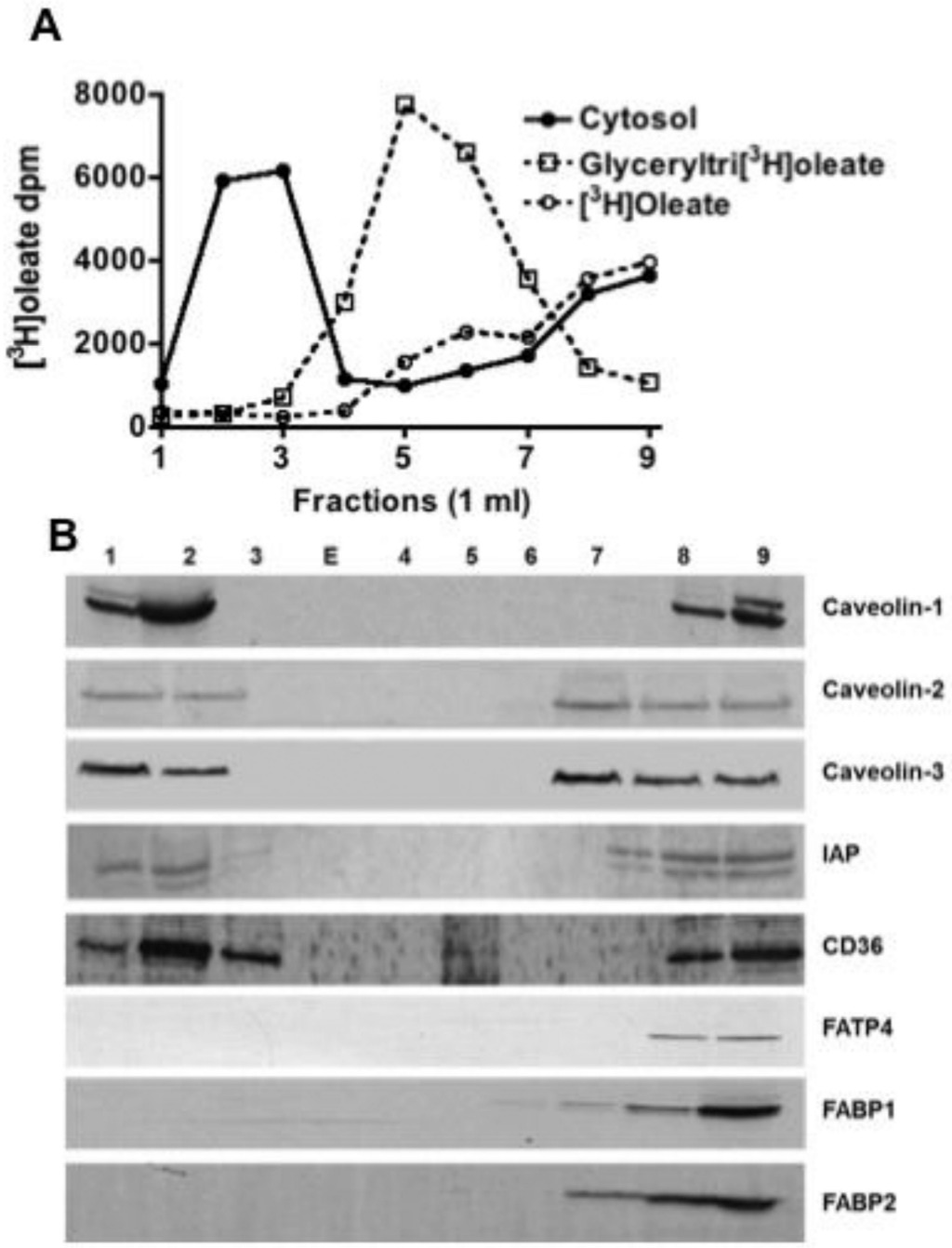

Fig. 4.

Absorbed ^{3}H-oleate is in a detergent resistant membrane fraction as shown by an OptiPrep gradient. A. Intestinal sacs were exposed to [^{3}H]oleate and the cytosol fraction prepared from enterocytes isolated from the sacs (Methods). Cytosol (1 mg) was treated with 1% Triton X-100 and placed at the bottom of a centrifuge tube containing an OptiPrep gradient (Methods). The gradient was centrifuged for 20 h and 1 ml fractions collected from the top of the gradient. The dpm were determined in each fraction (filled circles). Glyceryltri- ^{3}H-oleate (open squares) and ^{3}H-oleate (open circles) were separately dissolved in 1% Triton X-100, centrifuged, the gradient resolved, and the [^{3}H]-dpm determined for each fraction. The data are representative of 3 trials. B. Immunoblots (50 (μg prot) of each fraction from

the OptiPrep gradient were performed for the indicated proteins as shown to the right of the blots (Caveolin-1, Caveolin-2, and Caveolin-3, IAP, CD36, FATP4, FABP1, and FABP2). E indicates an empty lane.

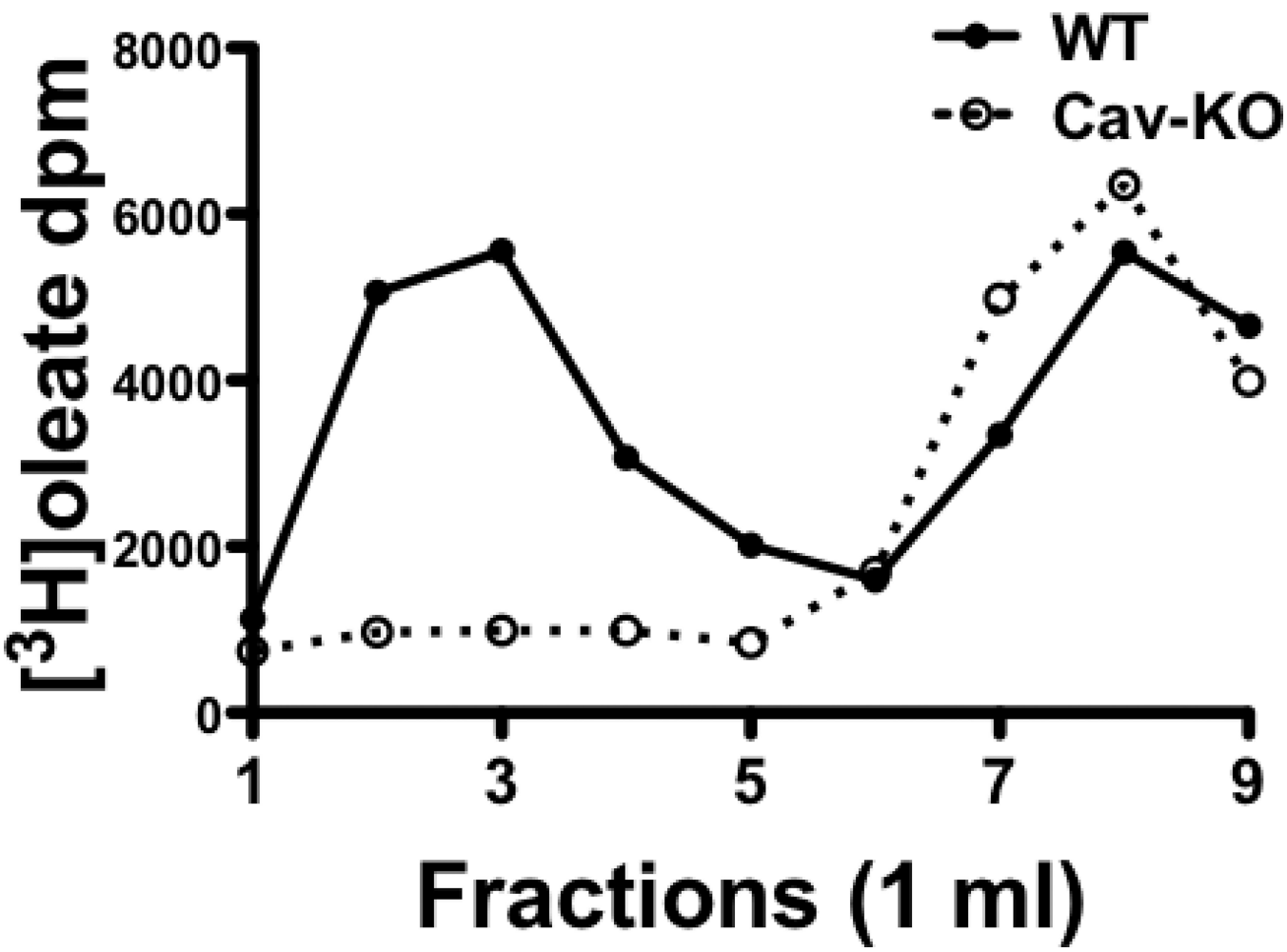

Fig. 5.

OptiPrep gradient distribution of absorbed oleate in the cytosol of WT and caveolin-1 KO mice. Cytosol was isolated from mouse intestinal sacks after incubation with ^{3}H-oleate for 2 min at 37°C (Methods). The cytosol was dissolved in 1% Triton X-100 and placed at the bottom of an OptiPrep gradient. The gradient was centrifuged for 20h and 1 ml fractions collected. WT is the cytosol preparation from wild type mice and Cav-KO from caveolin-1 gene disrupted mice. The data are the mean of 3 trials.

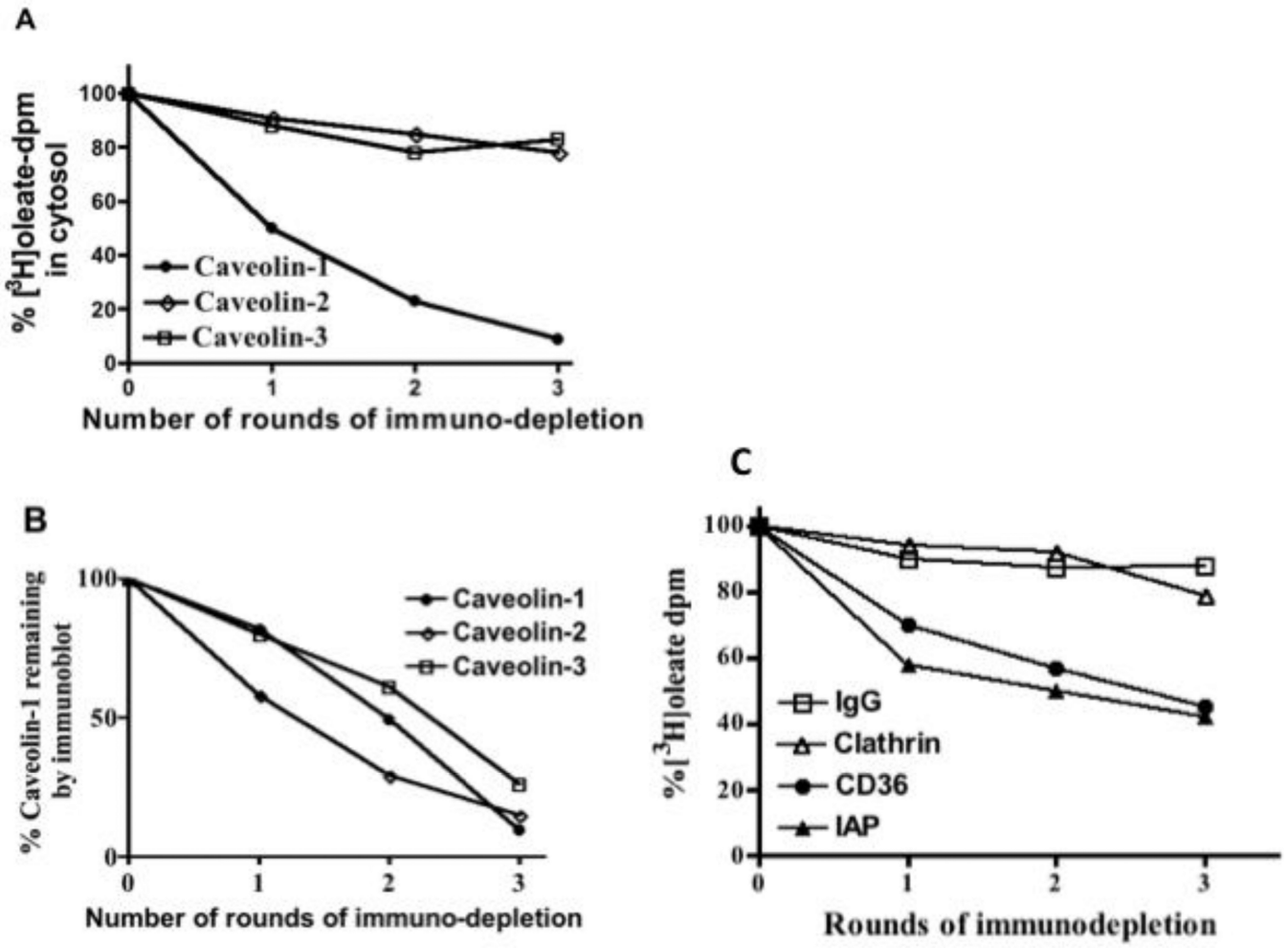

Fig. 6. Immunodepletion of caveolins and other proteins from the cytosol of enterocytes results in removal of absorbed [^{3}H]oleate. A. Enterocytes from intestinal sacs exposed to ^{3}H-oleate were collected, disrupted, and cytosol prepared (Methods). Cytosol (1 mg) was immuno-depleted of caveolin-1 (filled circles), caveolin-2 (open diamonds), and caveolin-3 (open squares) three times as indicated using specific antibodies bound to beads. After each round of immuno-depletion, the remaining ^{3}H-oleate was determined. The data are presented as a percentage of the ^{3}H-oleate at the start of the experiment and are representative of 3 trials. B. The optical density of the immunoblot band for Caveolin-1 after each round of immuno-depletion was determined (Methods) and the data presented as a percentage of the Caveolin-1 in native cytosol (filled circles). The band density of the immunoblots for Caveolin-2 (open diamonds) and Caveolin-3 (open squares) were measured after each round of immuno-depletion and the data expressed as a percentage of the amount present in native cytosol. Equal amounts of protein (50 μg) were loaded onto the gel. The data are representative of 3 experiments. C. Immunodepletion of various proteins from cytosol derived from intestinal sacs fed [^{3}H]oleate results in the partial removal of the ^{3}H-oleate. Enterocytes from intestinal sacs exposed to [^{3}H]oleate were collected, disrupted, and cytosol prepared (Methods). Cytosol (1 mg) was immuno-depleted of IgG (open squares), clathrin (open triangles), CD36 (filled circles), and IAP (filled triangles) three times using specific antibodies bound to beads. The remaining ^{3}H-oleate was determined after each round of immuno-depletion and the percent ^{3}H-oleate remaining as compared to the ^{3}H-oleate-dpm at the start of the experiment shown on the ordinate. After 3 rounds of immuno-depletion, nearly all of each protein was removed from the cytosol (IgG, 92 %, clathrin, 96%, CD6, 100%, IAP, 93%). Equal amounts of protein (50 μg) were loaded onto the gel. The data are representative of 3 trials.

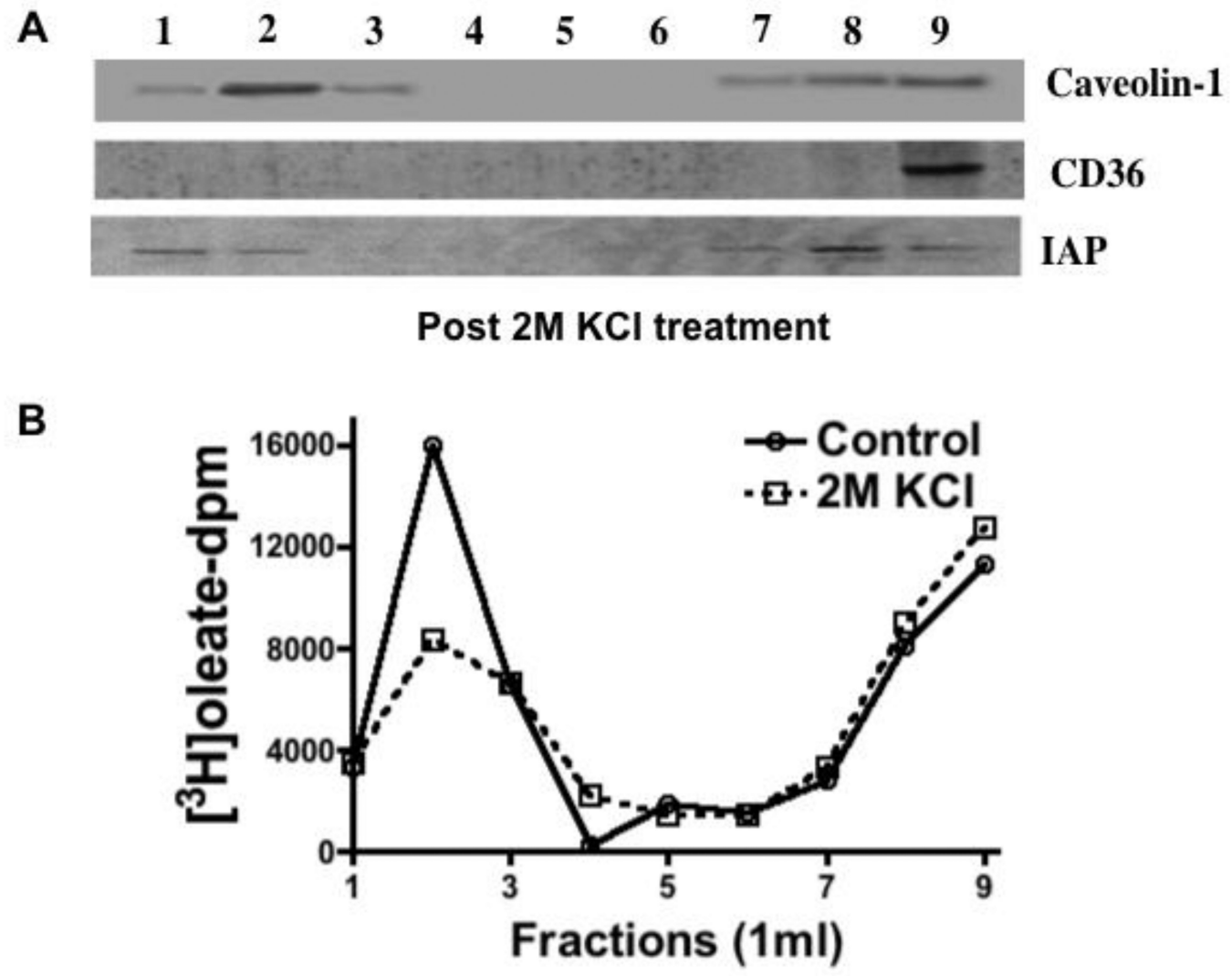

Fig. 7.

2M KC1 treatment of cytosol results in re-distribution of CD36 from the CEV to the DSF but caveolin-1 and IAP remain with the CEV. A. Cytosol from enterocytes isolated from intestinal sacs exposed to ^{3}H-oleate was treated with 2 M KC1. The cytosol (1 mg) was separated on an OptiPrep gradient and 1 ml fractions collected from the top of the gradient. Each fraction (50 μg prot) was immunoblotted for Caveolin-1, CD36, and IAP as shown. B. Intestinal cytosol (1 mg) from enterocytes isolated from intestinal sacs exposed to ^{3}H-oleate was made 2M with respect to KC1 or not and Triton X-100 added to a concentration of 1%. The treated cytosol was separated on an OptiPrep gradient and fractions (1 ml) collected from the top of the gradient. The ^{3}H-oleate dpm was determined for each fraction (Native cytosol [Control], open circles and 2 M KC1 treated cytosol [2 M KC1], open squares). The data are representative of 3 trials.

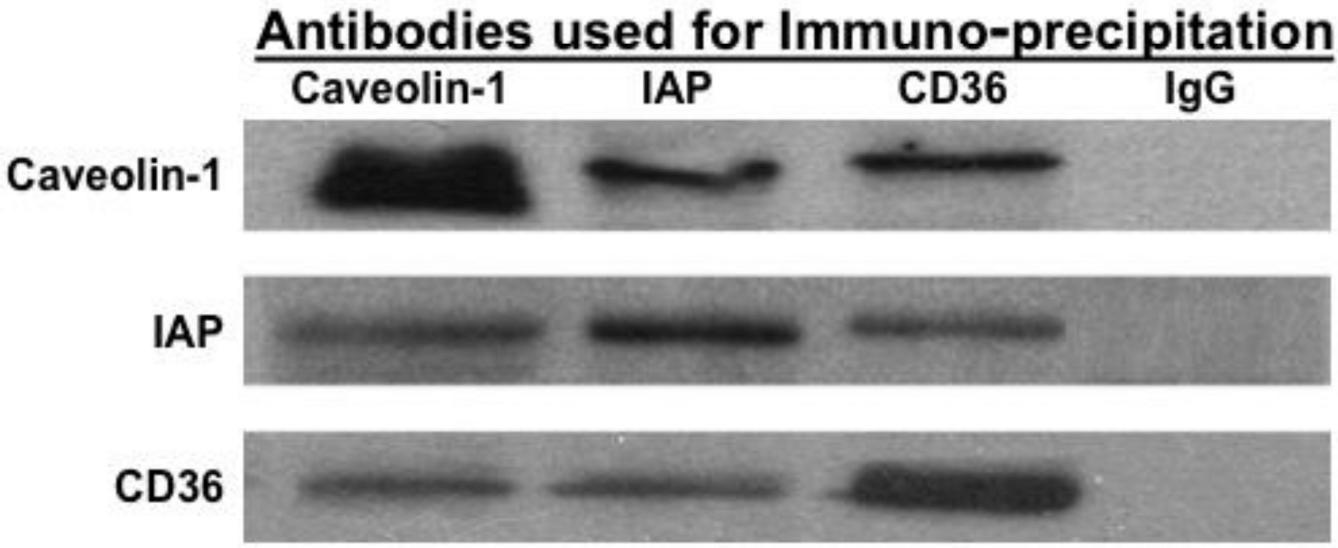

Fig. 8.

Caveolin-1, IAP, and FAT/CD36 are interactive in intestinal cytosol as shown by co-immuno-precipitation. Intestinal cytosol was incubated for 4h at 4 °C with rabbit anti-caveolin-1 or FAT/CD36 antibodies or goat anti-IAP antibodies bound to agarose beads. The beads were washed to remove unbound proteins (Methods), boiled in Laemmli's buffer, and the proteins separated by SDS-PAGE. The proteins were transblotted and immunoblots performed using the indicated antibodies. IgG bound to beads was used as a control (IgG).

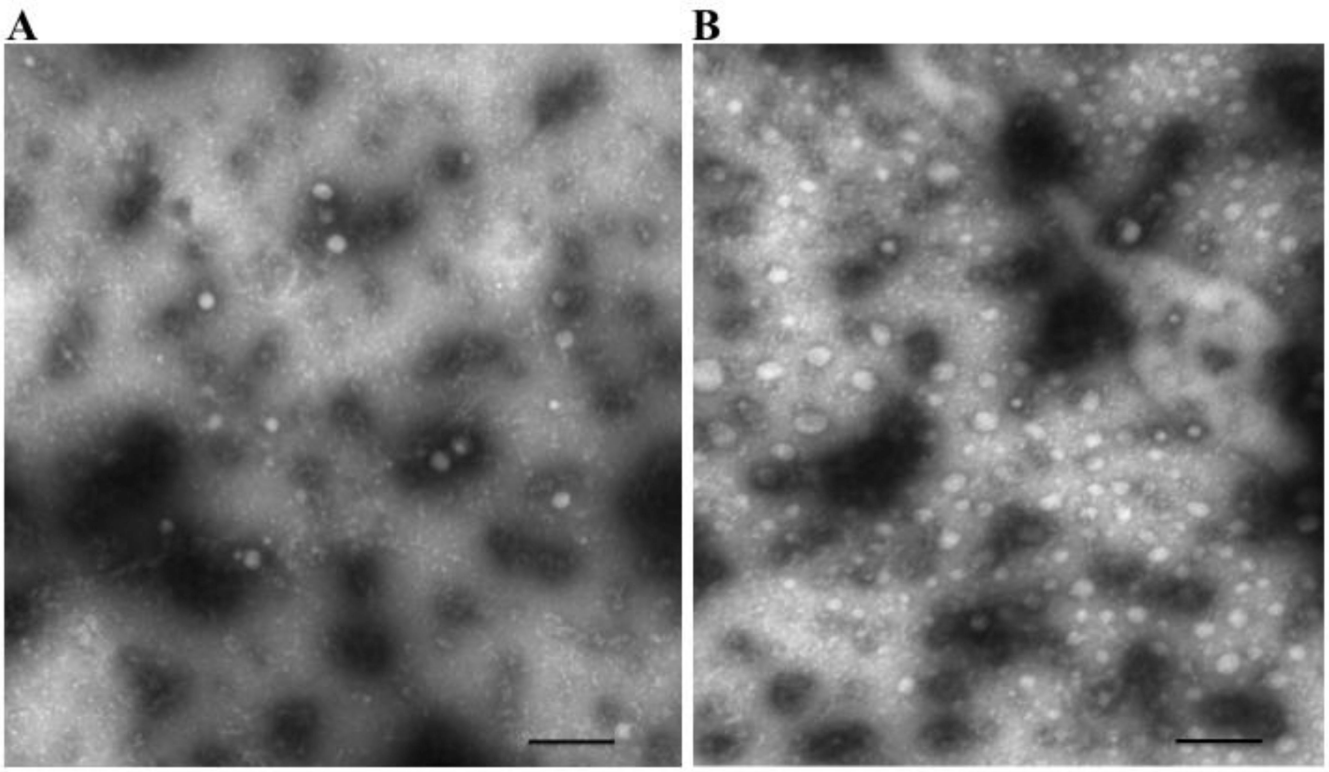

Fig. 9.
Electron micrograph of native cytosol isolated from enterocytes from rat intestinal sacs after exposure to no oleate (A) or 1 mM oleate bound to albumin (B). The negative staining technique was used and the grids examined using a JEOL electron microscope with an original magnification of 20,000 X (Methods). The bar at the bottom of the figure represents 500 nm.

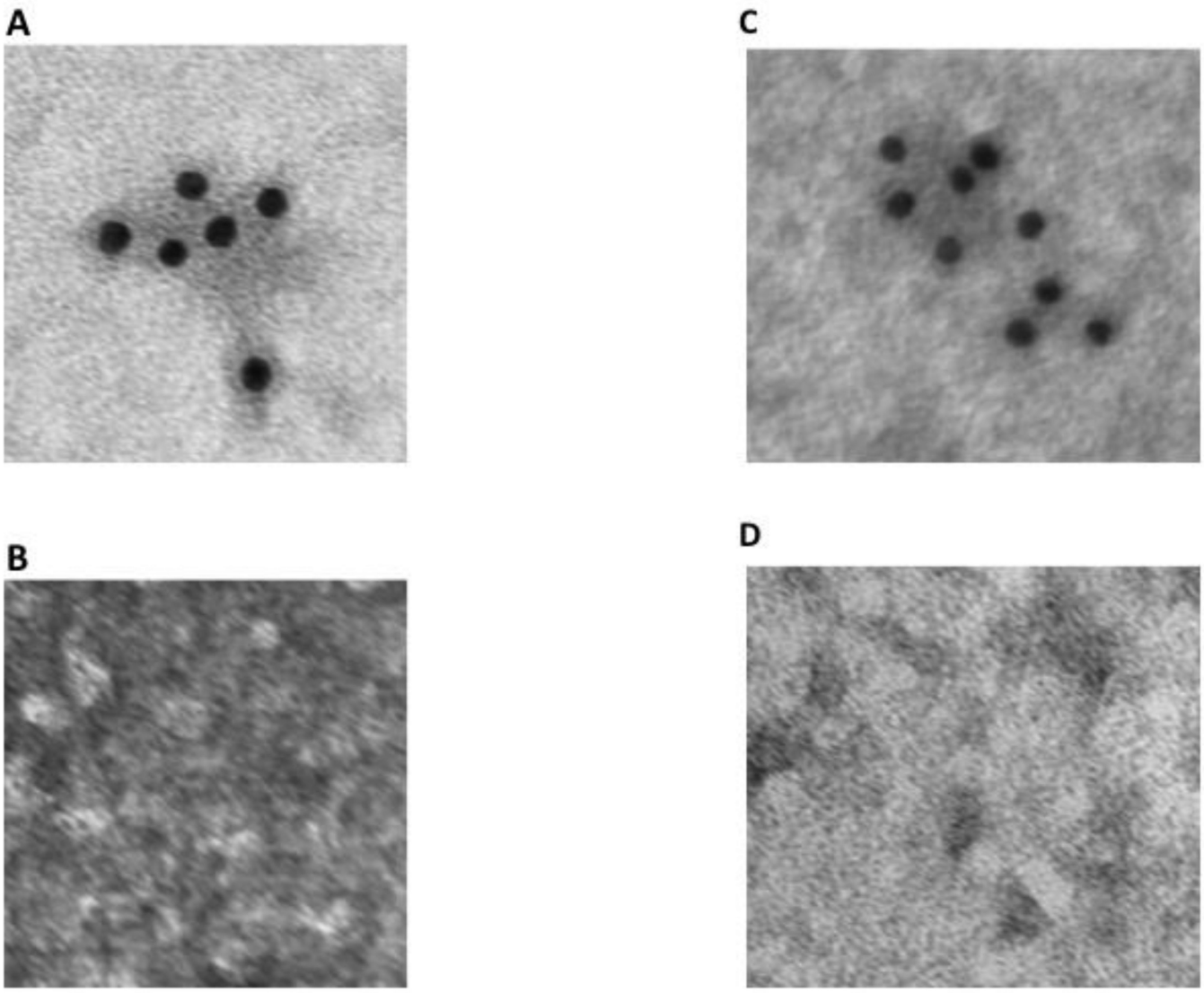

Fig. 10.

Immuno-electron-microscopy of native cytosol isolated from enterocytes derived from intestinal sacs exposed to no oleate (A and B) or 1 mM oleate (C and D) using antibodies to caveolin-1 or IgG. The negative staining technique was used and the grids examined using a JEOL electron microscope (Methods). In A and C, the grids were exposed to anti-caveolin-1 antibodies and subsequently to anti-rabbit-antibodies bound to 10 nm gold particles. In B and D, the grids were exposed to anti-IgG antibodies and subsequently to anti-rabbit-antibody bound to 10 nm gold particles. In each case the grids were washed to remove excess antibodies and then examined using the JEOL electron microscope with an original magnification of 20,000 X (Methods).

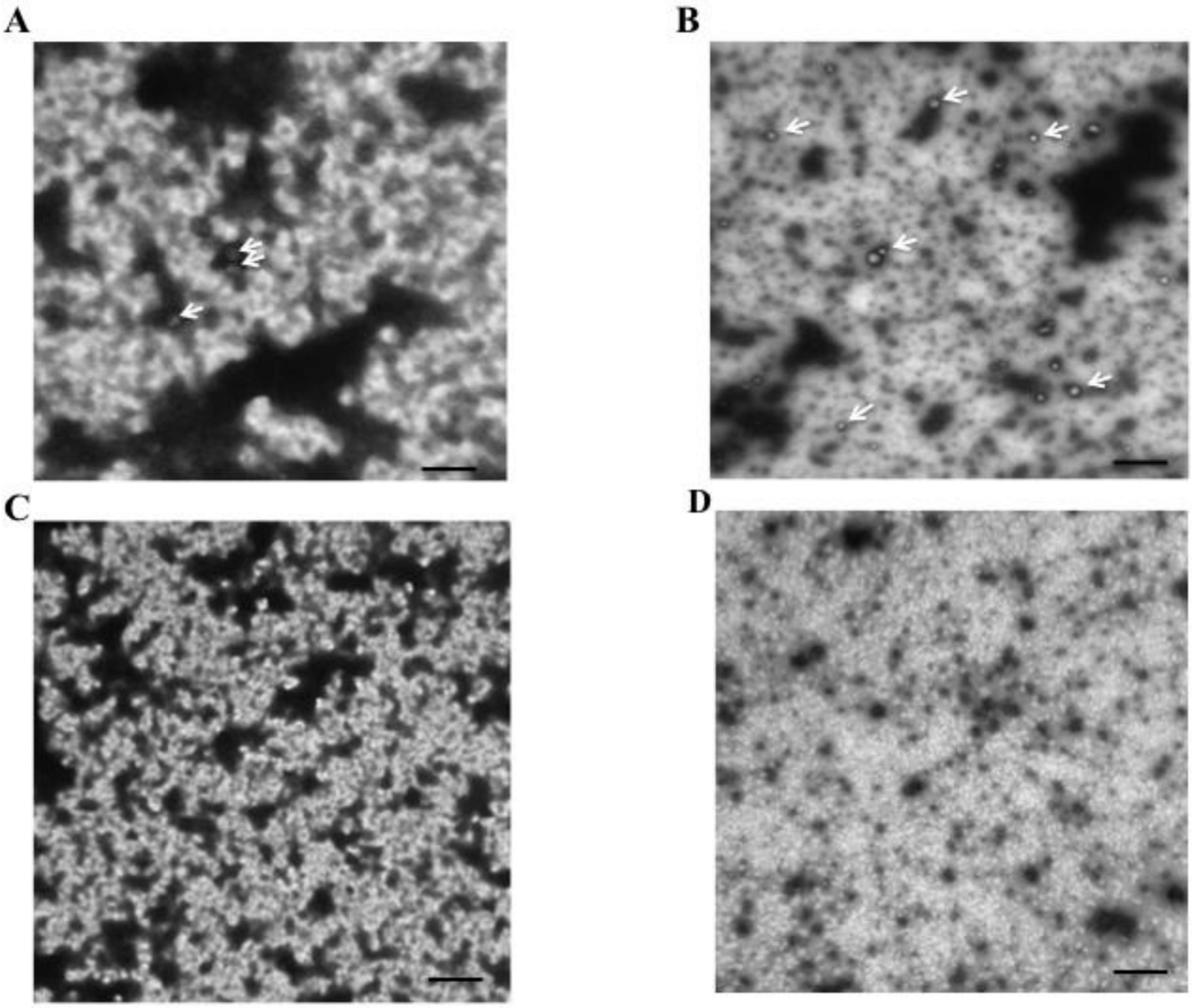

Fig. 11.

Electron micrographs of cytosol derived from enterocytes isolated from WT mouse sacs fed either no oleate (A) or 1 mM oleate bound to albumin (B). Enterocytes were exposed to either no oleate or albumin bound 1 mM oleate for 2 min and the cytosol harvested. The cytosol was placed on a glow discharged nickel grid and photographed at 20,000 X in a JEOL electron microscope (Methods). 3 vesicles (white arrows) are shown in A and 12 vesicles (6 identified by white arrows) are shown in B. Electron micrographs of cytosol derived from enterocytes isolated from caveolin-1 KO mouse sacs exposed to no oleate (C) or 1 mM oleate bound to albumin (D). No vesicles were identified either on no oleate or oleate feeding. The bar is 500 nm. The methods utilized are the same as in Fig. 10. 4 grids of each group were counted.

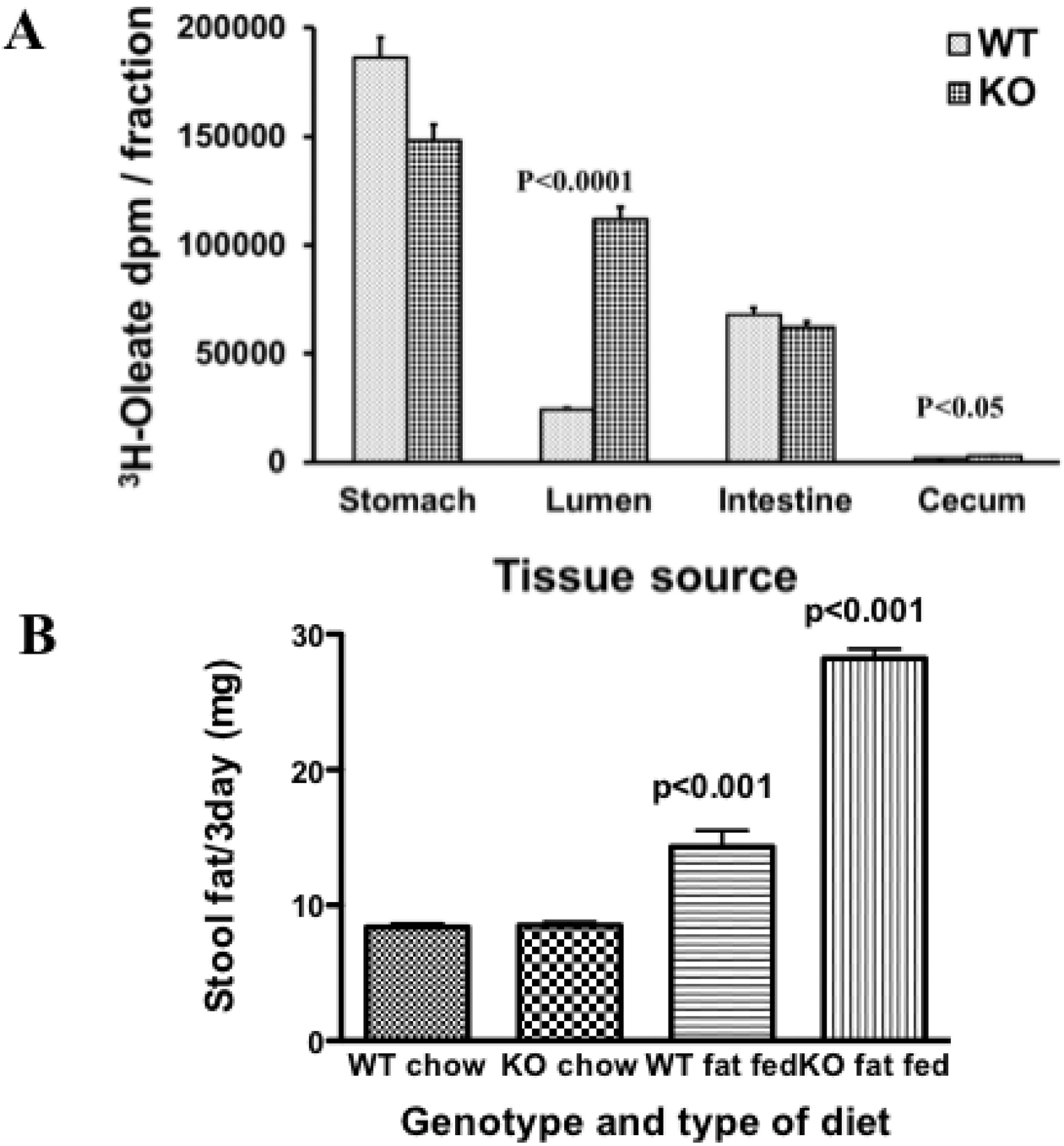

Fig. 12.

Absorption and intestinal distribution of dietary lipid in WT and KO mice. A. 0.2 ml corn oil supplemented with ^{3}H-oleate (4×10^6 dpm) was administered to WT and KO mice by gavage. After 30 min, the mice were anesthetized and the stomach, intestines and cecum removed. The intestine was flushed with taurocholate (10 mM) to obtain the luminal contents. The stomach and cecal contents and the whole minced intestine were separately collected, homogenized in 10 ml PBS and 100 μl obtained to determine radioactivity. The graph compares the ^{3}H-oleate dpm present in wild type (WT) to those present in caveolin-1 KO mice (KO) in the stomach, intestinal lumen, the whole intestine and cecum as indicated on the X axis. The error bars (±1 STD, N = 3) are indicated above each bar. Significant

differences between WT and KO mice are shown by the p values above the bars. B. Stool fat excretion in WT and caveolin-1 KO mice. 4 mice in each group were fed either a chow or a 23% fat containing diet as indicated on the X axis for 9 days. Stools were collected on the 7^{th} to 9^{th} day and pooled for fat analysis (Methods). The data shows the mean ± SD for each group. The p values above the bars represent differences in the means between the chow fed and the fat fed mice of each genetic type. The p value above the KO fat fed mice is also applicable in comparison with the WT fat fed mice. The stool fats were separated by TLC, stained with I_2, and the stained lipids compared to standards. 98% of the stained lipids were as FA.

Table 1

Enzymatic Activity of Cytosol Isolated from Enterocytes

	Enzyme Assayed (μmol/mg prot/min)			
Enzyme Source	G-6-P[a]	Sucrase	G-6PD[b]	Suc-D[c]
Whole homogenate[d]	0.77±0.08	0.87±0.1	0.23±0.02	0.23±0.03
Cytosol[d]	0	0.06±0.01	0.52±0.06	0

[a] Glucose-6-phosphatase

[b] Glucose-6-phosphate dehydrogenase

[c] Succinate dehydrogenase

[d] The data are the mean ± SEM (N = 4)